analytical chemistry

Review

pubs.acs.org/ac

Fiber-Optic Chemical Sensors and Biosensors (2013−2015)

Xu-dong Wang*,† and Otto S. Wolfbeis*,‡

†Department of Chemistry, Fudan University, 200433 Shanghai, P. R. China

‡Institute of Analytical Chemistry, Chemo- and Biosensors, University of Regensburg, D-93040 Regensburg, Germany

CONTENTS

High-quality optical fibers can be produced now at a low cost and large quantity, and this has further promoted the development of fiber-optic (chemical) sensors. After over 30 years of innovation, fiber-optic sensing technology has become more mature and popular because of acceptable costs, compact instrumentation, high accuracy, and the capability of performing measurements at inaccessible sites, over large distances, in strong magnetic fields, and in harsh environments. However, the technology is proceeding quickly in terms of innovation, and respective applications have been found in highly diversified fields. This Review covers respective work published in the time period between December 2012 and November 2015 and is written in continuation of previous reviews.[1] Data were electronically searched in SciFinder and MedLine. Additionally, the authors have collected references from various journals over the past 3 years.

However, a stringent selection of references had to be made in view of the number of articles published on fiber-optic chemical sensors and biosensors (FOCS). Priority has been given to FOCS for defined chemical, environmental, or biochemical species, to new schemes, and to new materials. This Review does not include (a) FOCS that obviously have been rediscovered; (b) FOCS for monitoring purely technical processes such as injection molding, extrusion, or oil drilling, even though these represent important applications of optical fiber technology, and (c) sensors for temperature and other physical parameters. Regrettably, the assignment of some articles to specific sections sometimes is somewhat arbitrary because some articles excel in terms of both new materials, advanced spectroscopic schemes, or analytical performance and selectivity.

Unfortunately, the term "sensor" has lost its clear definition over the past 10 years, and numerous articles are now published (mainly by organic chemists) where plain molecules ("molecular probes"; "indicators") are referred to as "sensors". However, the definition of chemical sensors (not only optical) is fairly unambiguous: *"Chemical sensors are miniaturized analytical devices that can deliver real-time and online information on the presence of specific compounds or ions in complex samples"*. The most attractive but challenging feature of sensors is to yield online information and to work in complex, often flowing samples and to provide continuous analytical information. Some of the so-called "sensors" published recently turn out to be conventional cuvette tests without any (online) sensing capability. Publication only seems to be justified by using the term "sensor" in the title; see the critical review by Wolfbeis.[2] It is also noted that certain authors seem not to be aware of the state of art in sensor technology and do not cite (or read?) existing articles in sensor journals and analytical journals.

Fiber optics serve analytical sciences in several ways. Plain fiber optics enable optical spectroscopy to be performed at sites

Special Issue: Fundamental and Applied Reviews in Analytical Chemistry 2016

Published: November 17, 2015

DOI: 10.1021/acs.analchem.5b04298
Anal. Chem. 2016, 88, 203−227

inaccessible to conventional spectroscopy, over large distances, or even on several spots along an optical fiber. Second, in being optical waveguides, fiber optics enable less common methods of interrogation, in particular evanescent wave spectroscopy and spatially resolved lifetime spectroscopy. Fibers are available now with transmissions over a wide spectral range.

Major fields of applications of FOCS are in sensing gases and vapors, medical and chemical analysis, molecular biotechnology, marine and environmental analysis, industrial production monitoring and bioprocess control, and the automotive industry. *Note:* In this article, sensing refers to a continuous process, while probing refers to single-shot testing. Both have their fields of applications. "Biosensors" based on immunoaffinity or polynucleotide interactions are unlikely ever to work in a fully reversible way, but respective devices have been termed biosensors for decades now (mainly by the medical and diagnostic community), and this terminology is accepted here.

FOCS are based on either direct or indirect (recognition-based) sensing schemes. In the first, the intrinsic optical properties of an analyte (such as its color, fluorescence, or chirality) are measured. In the second, the color or fluorescence of an immobilized indicator probe, a metal film or a (nano)material, or an optically detectable label is monitored. Another active area of research includes advanced methods of interrogation such as time-resolved or spatially resolved spectroscopy, evanescent wave and laser-assisted spectroscopy, (localized) surface plasmon resonance (SPR), leaky mode spectroscopy, and multidimensional data acquisition. Fiber bundles also have been employed for purposes of imaging, for biosensor arrays (along with encoding), or as arrays of nonspecific sensors whose individual signals may be processed via artificial neural networks. The use of advanced nanomaterials is growing rapidly and has led to impressive innovation.

BOOKS, REVIEWS, AND ARTICLES OF GENERAL INTEREST

A book on sol–gel optics[3] contains chapters on sol–gel fabrication of glass fibers for optics (written by K. Kamiya) and on index doped sol–gel films for fiber-optic chemical sensors. Optical methods for sensing and imaging of oxygen were reviewed.[4] Sections cover materials, spectroscopies, and applications. Intensity-modulated fiber-optic sensors for use in lumbar spine bending, upper and lower limb motion tracking, respiration, and heart rate monitoring was reviewed and assessed by Zawawi et al.[5] A highly competent review on plasmonic fiber-optic biochemical sensors was presented,[6] with a particular focus on recent methods for improving the limits of detection. Luminescent probes and (fiber-optic) sensors for temperature also were critically reviewed.[7] Edmonds[8] has edited a book on chemical sensors that also contains a section on chemical reagent-based fiber-optic sensors (written by A. L. Harmer and R. Narayanaswamy) and represents a valuable update of a former review on this subject.[9] Engineering metal oxide nanostructures on fiber-optic sensor platforms is critical for several reasons, and an effective integration scheme was presented for nanostructured tin oxide films for chemical sensing applications based on evanescent optical interactions.[10] The group of Grattan[11] has described the state of the art in fiber-optic sensor technology for measurement of relative humidity (RH) and moisture. A water-sprayable, thermogelating, and biocompatible polymer that may act as a host for fluorescent probes as used in chemical sensors was introduced.[12] Specifically, it was applied to fluorescent sensing and imaging of oxygen, pH values, and temperature.

SENSORS FOR (DISSOLVED) GASES AND VAPORS

This section covers all room-temperature gaseous species including their solutions in liquids. One major research focus is on hydrogen and methane because both are highly explosive when mixed with air. They can be sensed more safely with FOCSs than with electrical devices.

Hydrogen. Hydrogen (H_2; correctly: dihydrogen) is a clean and virtually inexhaustible source of energy. Its oxidation is producing water which is environmental friendly compared to fossil fuels. However, H_2 is gaseous at room temperature, has a very low density, and is difficult to store at high energy density, and its mixtures with air are highly explosive. In most cases, H_2 is compressed to a liquid at high pressure for easy transportation and storage. Hence, sensors for continuous and in situ monitoring are highly desired to detect hydrogen leakage. FOCSs for H_2 have the advantage of not having the risk of producing sparks, and distributed sensors may be used to monitor H_2 leakage at different sites along a transportation line.

Optical sensing of H_2, in most cases, is based on the strong affinity of dihydrogen for metallic palladium (Pd). By making use of this mechanism, different fiber-optic sensors were developed. An SPR-based fiber-optic H_2 sensor was fabricated by coating the unclad core of the fiber with layers of silver, silicon, or Pd.[13,14] The presence of H_2 in air causes changes of the dielectric properties of Pd and a shift in the resonance wavelength of the surface plasmons. The use of a silicon layer further enhances the shift. This sensor exhibits fairly good sensitivity in that 1% of H_2 in air can be easily detected. The presence of 4% of H_2 causes the resonance wavelength to shift by 11–12 nm. However, the SPR wavelength shift increases over time and becomes saturated after 40 min. This limits the application in real-time monitoring.

The same coating was used as a transducer layer in another type of hydrogen sensor. The layers were deposited on a multimode fiber whose cladding was partially removed.[15] The sensor is only sensitive to the transverse magnetic component of polarized light, while the transverse electric component can be used as a reference signal. The sensor performance strongly depends on the thickness of the layers in that the thickness of the silicon layer changes the resonant wavelength, while that of the silver and Pd layers govern sensitivity (LODs). The sensor works reversibly in the range of 0–4% of hydrogen (in synthetic gas) with a fast response (in 4–10 s), and changes of 0.5% of hydrogen can be accurately determined. The replacement of the silver layer by a gold layer in the coating did not significantly improve sensitivity.[16] A similar SPR sensor for H_2 was constructed by using a different composition of the coating.[17] Multilayer films of gold, tantalum pentoxide (Ta_2O_5), and Pd were uniformly coated onto the cladding of a heterocore structured optical fiber. The new coating significantly improved sensitivity in that a 28 nm shift in the SPR resonant wavelength is found at 4% of H_2 gas in nitrogen. The sensor has a typical response time of 15 s. A nanowire form of single crystal Pd–Au alloy was integrated with silica optical microfibers to produce a sensor for H_2 based on a Mach–Zehnder interferometer.[18] It uses an evanescent wave to excite surface plasmon polaritons, and the polaritons are propagated in suspended Pd–Au nanowires. This interferometer shows a high sensitivity to H_2 gas over a rather broad range (from 0 to 20% of H_2) and yet needs 1 nW of power only for operation.

DOI: 10.1021/acs.analchem.5b04298
Anal. Chem. 2016, 88, 203–227

Reflectometry is a well established, reliable, and yet simple spectroscopic method for use in chemical sensing. A reflection-based FOCS for H_2 was fabricated by deposition of a thin film of Pd−Au alloy acting as a hydrogen-sensitive layer on an optical fiber.[19] Reflectivity of Pd decreases with increasing hydrogen pressure. The response time is less than 15 s, and the sensor can continuously and quantitatively measure H_2 pressures of up to ∼250 mbar. Oxygen and methane do not interfere, but CO interferes even at a concentration as low as 19 ppm. The same sensor was used to determine H_2 partial pressure in natural gas, and the carrier gases methane, ethane, and propane, as expected, did not interfere.[20] Another FOCS for determination of H_2 dissolved in oil was developed using a PTFE-Pd-capped Mg−Ti thin film (Figure 1).[21] The sensor

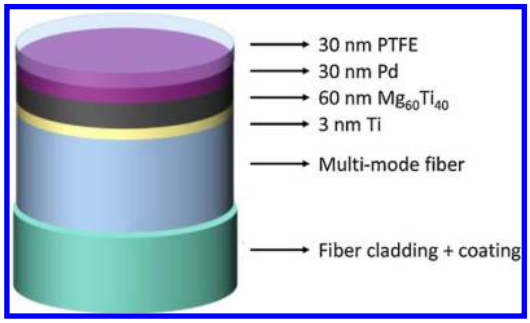

Figure 1. Schematic of the PTFE-Pd-capped magnesium−titanium thin film coating for constructing a fiber-optic hydrogen sensor. (Reprinted from *Sens. Actuators, B*, Vol *190*, Mak, T.; Westerwaal, R. J.; Slaman, M.; Schreuders, H.; van Vugt, A. W.; Victoria, M.; Boelsma, C.; Dam, B. Optical fiber sensor for the continuous monitoring of hydrogen in oil, pp. 982−989 (ref 21). Copyright 2014, with permission from Elsevier.)

also works in the reflection mode and can measure dissolved H_2 in the 5−1500 ppm concentration range depending on the operating temperature. The working range increases with operating temperature. Again, oxygen and methane do not interfere, but CO does.

The introduction of a fiber Bragg grating (FBG) into optical fibers strongly increases analytical accuracy and renders respective sensors more sensitive. An FBG hydrogen sensor was fabricated by coating the FBG with a film consisting of a Pd/Ag polyimide composite.[22] Again, dissolved H_2 was measured in power transformer oil, and a sensitivity, expressed as the wavelength shift (in pm) per μL of H_2 dissolved in 1 L of oil sample, as good as 0.050 pm is reported. It can be operated at temperatures up to 80 °C but at the expense of sensitivity, while response times are significantly improved. Another FBG sensor for H_2 is making use of a Pd/SiO_2 film as the sensor layer.[23] It can accurately quantify H_2 in concentrations down to 0.1% in dry air within less than a minute. Similar to the Pd/SiO_2 sensing film, nanoparticles consisting of a Pd−Au alloy and incorporated into a thin film of SiO_2 also are sensitive to H_2.[24] The sensor performances of the Pd/SiO_2 and Pd−Au/SiO_2-based sensors were compared at varying temperatures. Both have a fully reversible response to H_2 in the range of 0−100%, but the Pd/SiO_2 sensor has a higher sensitivity. The sensitivity of both sensors decreases with increasing temperature. Improved sensitivity was achieved by coating an etched FBG with Pd/Ag composite film.[25] When exposed to 4% of H_2, this sensor exhibits a wavelength shift of 40 pm.

Wang et al. described a Fabry-Pérot interferometer (FPI) sensor using a single-mode fiber for H_2 sensing.[26] The FPI cavity was fabricated by femtosecond laser micromachining near the distal fiber end and then coated with a Pd film. The interferometer output spectrum shifts for 10, 30, 100, and 150 pm at the H_2 concentrations of 2%, 4%, 6%, and 8%, respectively. The sensor is compact and easy to fabricate. Chowdhury et al.[27] created a self-referenced optical fiber refractometer for H_2 using a ball lens acting as the sensor head. A 350 μm ball lens was created at the tip of a single mode fiber and then coated with a 40 nm layer of Pd. The reaction of Pd with hydrogen changes the reflectivity of the coating, and the intensity of the reflectance can be related to the concentration of H_2. Response is linear in the 0−1% concentration range, and the detection limit is 10 ppm in air. This technique represents a remarkably simple sensing arrangement, and a sample area that is ∼40 times larger than that of a typical single-mode fiber core.

The composition of the Pd coatings appears to play a decisive role in the performance of sensors for H_2. Recently, a Pd−Y film was reported to display an even better performance than the Pd film. A fiber-optic Fabry-Pérot sensor was constructed where the fringe contrast is measured as a function of the concentration of H_2 between 0 and 5.5%.[28] The use of a Pd−Y alloy also results in improved permeability for H_2 compared to other Pd-based alloys, but suffers from aging on air. Thermal annealing of the alloy can improve the situation,[29,30] and less than 5% drift of the zero H_2 signal is observed when cyclic between adsorption and desorption of H_2. The FOCS based on annealed Pd−Y alloy can detect H_2 in concentrations down to 0.1% in nitrogen, and the analytical range is up to 2%.

Other recent Pd-based sensor materials include a ZnO/Pd nanocomposite which has a much higher sensitivity than a layer-by-layer coating.[312] ZnO and Pd were alternatingly deposited by a layer-by-layer technique on the fiber core. Another SPR-based fiber-optic sensor for H_2 uses the nanocomposite combined with a layer of silver and showed a 7-fold improvement over the sensors based on a layer-by-layer coating. The former exhibits a shift in resonance wavelength (at 4% H_2) as large as 139 nm, while in the latter it is only shifted by 20 nm.

It was known that oxygen, moisture, and CO can interfere in H_2 sensors based on using a Pd metal surface. Szilágyi et al.[32] have suggested the use of a metal−organic framework (MOF) architecture to improve selectivity. The copper(II) salt of 1,3,5-benzenetricarboxylic acid was chosen as the MOF material. It was deposited on the Pd layer as a protective layer, again via a layer-by-layer technique. Results showed that the protective coating did not adversely affect the H_2-sensing properties. However, the MOF layer did not substantially improve selectivity in that water vapor; oxygen and CO still interfere to some extent. The authors pointed out that, if the pore size of MOF is in a suitable range, it may act as a selective coating for hydrogen sensing.

WO_3 is the second kind of main material that is often used in optical sensing of H_2. A new sensing scheme using a WO_3 film and Pt metal as a catalyst was described by Li et al.[33,34] Here, the color of the WO_3 film changes to dark blue if the film is exposed to H_2 gas. Consequently, the refractive index (RI) of the WO_3 film decreases and absorbance increases. The changes observed in reflectivity can be related to the concentration of H_2. The deposition of the sensing film on an optical fiber produced a reflection-based FOCS for H_2. The detection

DOI: 10.1021/acs.analchem.5b04298
Anal. Chem. 2016, 88, 203−227

system consists of a dual-path designed to eliminate most noise resulting from fluctuations of light source, but also for fiber losses and effects of temperature. The sensor has a nonlinear response to H_2 in concentrations between 0 and 4% (v/v). Its sensitivity is best at low concentration (up to 0.5%), which makes the sensor quite suitable for sensing a low level of H_2. Another optical sensor for H_2 uses an ultrathin layer of copper sulfide that incorporates Pd metal.[35] After exposure to H_2, the color of the film gradually changes from dark green to brown, and this can be easily read by bare eyes. An instrumental signal is obtained by measurement of absorbance (and, conceivably, reflectivity) in the near-infrared region. Absorbance decreases with ascending concentration of H_2, and up to 0.8% of H_2 gas in air can be detected. Such sensors can be produced on flexible transparent supports and at rather low cost.

Yang and colleagues[36−38] have reviewed and compared the sensing performance of optical fiber hydrogen sensors with Pd-based thin film and sol−gel WO_3 coatings. They found that side-polished fiber Bragg grating (FBG) sensors possess improved sensitivity. Sensors based on thin Pd film coatings are particularly well reversible and reproducible. They also are compact, inexpensive, easily manufactured, and most suitable for detecting H_2 leaks. In comparison, sensors based on sol−gel WO_3 coatings exhibit higher sensitivity. More importantly, they are not interfered by relative humidity (RH), methane, and CO which are known to affect Pd-based sensors. The same group later combined both techniques to produce an FBG H_2 sensor by employing a Pt-loaded WO_3 coating.[39] This resulted in an improved sensitivity that can reach up to a 536 pm wavelength shift at a 10 000 ppm level of H_2. The detection threshold is 200 ppm. This sensor is not interfered by RH, CH_4, and CO.

Not many other H_2-sensitive materials are known. Jiang et al.[40] reports on a highly sensitive FOCS for H_2 gas that works at relatively high temperatures. The sensor is making use of a long-period fiber grating coated with a proton-conducting $SrCe_{0.8}Zr_{0.1}Y_{0.1}O_{2.95}$ (SCZY) nanocrystalline thin film and a chemically inert and thermally stable nanoporous silicalite protective layer. This material is capable of measuring H_2 partial pressure at 500 °C in the range between 0 and 100% by virtue of measuring the transmission spectrum shift. The sensitivity is increasing with increasing thickness of the SCZY film but decreases with increasing thickness of the silicalite film. Its high sensitivity and good reversibility render the sensor suitable for monitoring H_2 gas at high temperature, especially in industry plants and engines.

Hydrocarbons. Hydrocarbons usually are detected via their weak absorption in the infrared (IR) between 2900 and 3000 cm^{-1}. Sensors for methane (CH_4) are needed in the gas and oil industry in general, as detectors for natural gas in homes and in industry, in coal mines, and in studies related to the greenhouse effect of methane gas. CH_4 has a relatively strong adsorption at 1.6 μm, and this is routinely exploited for the quantification of this important gas. A fiber-optic sensor for CH_4 was constructed using a distributed feedback laser diode along with a harmonic detection technique.[41] A sequential multipoint sensor for measuring average methane concentrations was developed by connecting several gas cells in series via single fiber optics.[42] The absorption of methane at 1666 nm was employed because this can circumvent any interferences by water vapor and certain other gases. The system only needs a single distributed feedback laser source and only one detector. It does not require multiplexing techniques to distribute the laser intensity among multiple gas cells. The 2*f* amplitudes in the near-IR increased with the methane concentration, and methane can be quantified in the 0−10% (v/v) range with linear response. CH_4 can be sensed in the 0 to 20% concentration range with adequate sensitivity. The detection system shows good dynamic response and stability, which can be used for distributed CH_4 in coal mines and along pipelines. In order to improve analytical precision, an FOCS based on the use of a tunable diode laser was designed.[43,44] The sensor employs a 2*f* wavelength modulation spectroscopy measurement scheme. It can measure CH_4 in the range of 2.0−50 ppm (v/v) with a remarkable precision of 1.36 ppm. The detection limit is as low as 1.56 ppm. However, the sensor suffers from its long configuration that includes a 6 m single-mode optical fiber. Another CH_4 sensor was reported that exploits SPR and is making use of a composite consisting of graphene, carbon nanotubes, and poly(methyl methacrylate) as a coating for the cladding of the fiber.[45] When exposed to CH_4, a longwave shift in the resonance wavelength can be observed that increases with increasing concentration of CH_4. The analytical range extends from 10 to 100 ppm. The sensor fabricated using the hybrid composites shows up to 30 nm of total shift in resonance wavelength, which is much higher than other sensors based on the use of graphene-carbon nanotubes, carbon nanotubes, or reduced graphene oxide (rGO).

A refractometric FOCS for direct measurement of toluene vapor without any other adsorption layers was also described.[46] The fiber contains a short section of suspended core microstructure. The inner structure consists of a relatively thin silica core fiber (2.6 μm) which is surrounded by three large cladding holes with radii of 26 μm. This architecture was chosen in order to allow CH_4 gas to flow through the microstructure. The spectral attenuation of the sensor in the 1400−1650 nm spectral range serves as the analytical signal, and the output power decreases as the concentration of toluene vapor increases. The sensor has a good sensitivity (in the toluene concentration range of 0−1.2 mol %), and, hence, also works at the explosion limit. The detection limit is as low as 0.0079 mol %.

Oxygen. Sensing oxygen (O_2) is one of the most successful fields of FOCS technology. Several companies have emerged in the last 15 years. Their sensitivity, selectivity, and small size make such sensors highly attractive. All commercial sensors are based on measurement of the quenching of luminescence by O_2. Quenching is typically measured via changes in decay time, and sensor modules can be as small as a USB stick. A comprehensive review summarizing the state of the art in terms of optical probe for O_2, (polymeric) materials for hosting probes, and sensing/detection schemes has appeared.[4] A survey on fluorescent probes for oxygen sensing also was given.[47] A shorter review on the essential features of commercial (fiber-optic) sensors for O_2 (along with a discussion of commercial products) also has been published,[12] and the author concluded that optical sensors probably will displace almost 70% of the commercially available amperometric sensors for O_2, all based on the use of Clark electrodes.

The combination of various oxygen sensitive probes and hosting materials enables the development of fiber-optic sensors with different sensitivities to O_2. An evanescent wave sensor for O_2 was obtained by dip-coating an unclad optical fiber with fluorinated organically modified silicate (ormosil) doped with the fluorescent and quenchable probe Ir-$(piq)_2(acac)$.[48] The ormosil was prepared from 3,3,3-trifluoropropyltrimethoxysilane (TFP-TriMOS) and *n*-propyl-

DOI: 10.1021/acs.analchem.5b04298
Anal. Chem. 2016, 88, 203−227

trimethoxysilane (n-propyl-triMOS) and exhibits high permeability to gas. The evanescent wave field produced in the fiber core was used to excite the oxygen-quenchable fluorophore, and the intensity of fluorescence was used as analytical signal. The sensor has a typical response time of 1 s, and such a short response time allows for real-time monitoring of human breath gas. Chen et al.[49] have varied the response and performance of optical fiber sensors for O_2 by variation of the host polymer. Three acrylate polymers, viz., poly(methyl methacrylate) (PMMA), poly(ethyl methacrylate) (PEMA), and poly(propyl methacrylate) (PPMA), were used as the matrix for immobilizing the indicator Pt(II)octaethylporphyrin on the tapered end of a polymer optical fiber. The oxygen sensitivity increases in the order of PMMA < PEMA < PPMA, and the typical response time decreases in the same order. Sensors produced using the PPMA as matrix possess the highest sensitivity and fastest response time (<100 ms). However, PtOEP is not a state-of-the art probe for O_2. The addition of an ionic liquid during production of electrospun polymer host improves sensor stability.[50] Unlikely in the coating technique, O_2-sensitive indicators can be directly immobilized in a fiber during tapering. Pulido and Esteban[51] have described such a method for preparing a highly reproducible sensor for O_2. By immobilizing two fluorophores (one being inert and acting as a reference dye) during the tapering process, ratiometric measurement of oxygen can be easily achieved and represents an alternative to the more common methods based on measurement of decay times.

Fiber-optic sensors have the attractive feature of allowing measurements to be performed at sites that are inaccessible to conventional methods of analysis. An O_2 sensing structure was placed inside a microfluidic device in a capillary optical fiber (COF) with a ring-shaped waveguide.[52] The inner surface of the waveguide in the COF was coated with an oxygen sensitive layer incorporated with the oxygen indicator $Ru(dpp)_3$ and, unlike in previous COF sensors for O_2, fluorescein was added as an inert reference dye. Oxygen gas can freely flow through the COF, and only 0.20 μL of a gas sample is required for sensing gaseous O_2. The sensor has a linear Stern−Volmer plot in the oxygen concentration range from 0 to 100%. The response time is ∼7 s. Kazemi et al.[53] have developed a fiber-optic system to detect O_2 leakage in harsh environments such as in the engine section of a Boeing Delta IV launch vehicle. A ruthenium-based fluorescent indicator was covalently immobilized on a porous glass rod, which was then placed at the end of multimode fiber. Blue light from an LED is guided into the fiber and used as excitation source, and the fluorescence emission intensity is related to the O_2 concentration in the range of 0−10%. The sensing system has good reliability and, in contrast to earlier blue LED-based sensors for O_2, can compensate for temperature fluctuations. The system responds fully reversibly, and it takes only 1−5 s to analyze a sample. Hence, it allows real-time monitoring of O_2 leakage on the launch vehicle. Such sensors measure oxygen along the length of an optical fiber which, in the best cases, was reported to be as long as 1 km. Distributed sensors for O_2 have been long known and usually are based on time-domain reflectometry. In order to achieve good spatial resolution, probes with relatively short decay times are preferred. The fluorescent O_2-probe triangular-[4]-phenylene (with an unquenched decay time of 86 ns) was immobilized at the fiber tip.[54] This short decay time enables sensing with a spatial resolution of some meters, and the maximal length of the fiber is around 90 m which is adequate from many industrial and biotechnology applications. The analytical range extends from 0 to 200 mbar, but in the configuration used maximally, two sensor points can be measured at the same time.

The precision of all optical sensors, and of sensors for O_2 in particular, is affected by temperature (T), and this represents a serious source of error. Thus, one has to compensate for the influence of T. One solution in an all-optical sensing system involves the use of a T-sensitive indicator probe together with the O_2 indicator. Such a "dual sensor" was developed by coating the end of an optical fiber with fluorinated xerogels doped with PtTFPP and 5(6)-carboxyfluorescein.[55] Both fluorophors can be simultaneously excited using a 405 nm LED, and the ratio of two emissions detected and used for ratiometric determination of O_2. The fluorescence intensity of this fluorescein is linearly related to T in the range between 25 and 66 °C. The effect of T can be compensated for in this way. The same configuration was later used to fabricate a sensor for dual sensing of oxygen and the Cu^{2+} ion by replacing 5(6)-carboxyfluorescein with CdSe quantum dots.[56]

Small-sized lasers are available for almost all wavelengths in the longwave UV, visible, and near-IR nowadays. Their intensity, spectral purity, low divergence, and coherence make lasers the preferred light source in fiber-optic sensing. The use of lasers on one hand can improve the limit of detection. On the other hand, strong lasers can cause photodecomposition of indicators. A third source of error when using strong lasers results from the fact that sensor layers are rather thin and decay times of practically all probes are rather long. Hence, strong laser excitation may cause the fraction of excited-state molecules to be larger than that of ground-state molecules. This will adversely affect the O_2 sensing performance. The groups of Borisov and Klimant have shown that strong light intensities will cause a strong population of the excited state of the luminophore, and this has resulted in a nonlinear relationship between the intensities of excitation light and luminescence.[57,58] If very bright indicators are used, for example, PdTPTBPF, the bias can be as high as 50% when using strong lasers for photoexcitation. Thus, it cannot be generalized that it is always(!) better to use strong photoexcitation. Another ratiometric oxygen sensing system is based on gadolinium labeled hematoporphyrin monomethyl ether (Gd-HMME) and filter paper.[59] The ratio of the constant (blue) fluorescence of the filter paper and of the O_2-dependent yellow phosphorescence of Gd-HMME is measured. The detection limit is 0.01% (v/v) of O_2, and the response time is 4 s.

Spatially resolved oxygen patterns were acquired via a multiplexing fiber-optic microsensor system based on established sensor chemistries.[60] An open and low-cost optical-fiber system for the quantitation of O_2 uses a multifrequency phase-resolved method.[61] Data processing and evaluation is based on quadrature detection (also known as the I/Q method) very much like in the first lifetime-based sensor of that kind published back in 1986. All data are digitally processed. The probe [Pt(II) meso-tetra(pentafluorophenyl)porphine] was placed in an oxygen-permeable polymer. The proposed sensor system has a measurement accuracy of <0.2 kPa over the measurement range of 0−20 kPa. Finally, sensors with extremely low sensitivity for O_2 were described by various groups using either highly permeable host polymers[62] or highly sensitive fullerene probes.[63]

DOI: 10.1021/acs.analchem.5b04298
Anal. Chem. 2016, 88, 203−227

Carbon Dioxide. Carbon dioxide (CO_2) is a notorious green-house gas, one of the causes for global warming, and an essential buffer component in seawater and blood. Hence, CO_2 is sensed both in the gaseous phase and in the dissolved form. Similar to methane, CO_2 has a fairly strong infrared adsorption band peaking at 1.57 μm, and this can be employed to direct sensing of CO_2.[64] A fiber-optic CO_2 monitoring system was developed on the basis of tunable diode laser adsorption spectroscopy and distributed feedback laser and then applied to monitoring CO_2 in a coal mine. CO_2 concentration was calculated using a least-squares fitting method. The system is capable of measuring CO_2 levels as low as 0.05% (v/v) with good accuracy and stability. However, methane strongly interferes, which is problematic in the case of coal mines. In another kind of FOCS for CO_2, a fiber was coated with a clad composed of polydimethylsiloxane (PDMS)[65] which acts as a kind of preconcentrator for the gas. The sensor also exploits the adsorption at around 1.57 μm for detection. Another sensor of that kind only differs by the analytical wavelength (2.7 μm)[66] and was applied to monitor CO_2 in recirculating exhaust gas in diesel engines. The sensor has a very fast response (0.15 s), and IR absorbance is linearly related to CO_2 concentration in the range from 0 to 10%. A hollow-core photonic bandgap fiber transmitting at 2 μm was used in a compact CO_2 monitoring system.[67] The absorption line of CO_2 at 2005.09 nm was used to quantify the gas. The sensor system exhibits a linear response in the gas pressure range from 50 to 600 hPa.

CO_2 cannot be detected by the IR method in a water solution because of the strong interference by the OH vibrations of water. However, CO_2 forms a weak acid (carbonic acid) when dissolved in and partially reacting with water. Hence, the concentration of CO_2 may also be deduced from the increase in the acidity of an aqueous sample. The change in pH can be detected by using an optical indicator. There is much prior art, and such sensors also are commercially available. For example, a long period grating FOCS for CO_2 was described that uses a polymeric sensitive layer that contains a slightly alkaline buffer whose acid–base equilibrium changes on exposure to CO_2 and also contains the yellow indicator 4-nitrophenol.[68−70] The sensor layer changes its color (it becomes colorless on exposure to CO_2). In addition, the RI changes and this induces a shift of the resonance wavelength of the long period grating. The resonance wavelength shifts 180 pm when the CO_2 concentration increase from 0 to 30%. The typical response time of the sensor is 12 s. Such sensors have a good reversibility but can dry out.

Nitrogen Oxides. Atmospheric nitrogen dioxide and ozone are notorious pollutants, and substantial interest in respective sensors therefore has arisen. Both electrochemical[71] and optical sensors are in use. An optical fiber bundle was coated with a cellulose acetate film doped[72] with fluorescent diaminobenzoacridine. This compound has a weak fluorescence that is enhanced on reaction with NO to form a triazole in the presence of molecular oxygen. The sensor is capable of measuring NO in concentrations between 10 nM and 10 μM, with a detection limit of 1.0 nM. Response is, however, irreversible. The same group later observed that the fluorescence of CdSe quantum dots is quenched on chemical reaction with NO.[73] Nitric oxide reacts with dissolved oxygen in water and coordinates to Cd^{2+}, and this causes quenching of the fluorescence of the quantum dots. On the basis of this finding, a sensor for NO was therefore developed that can sense NO in the range between 0.1 and 1.0 μM with a 10 nM detection limit. Again, fluorescence quenching is caused by an irreversible chemical reaction.

Optical fiber sensors for NO_2 were also reported. A reversible optical fiber sensor was obtained by coating a multimode fiber tip with a thin film of the lutetium(III) bisphthalocyanine complex ($LuPc_2$).[74] After exposure to NO_2, the absorption of the sensor film at 660 nm is drastically decreased, but the response is fully reversible. The sensor can monitor NO_2 in the 0−5 ppm concentration range with a resolution of 0.2 ppb. Recoveries at low NO_2 levels are rather long, but can be accelerated by placing a UV light source emitting at 365 nm above the sensor film. UV radiation promotes the photodissociation of the complex formed between NO_2 and $LuPc_2$. As a result, the sensor recovers within <30 min.

Other Gases. A fiber-tip photoacoustic sensor for acetylene (C_2H_2) was designed[75] where the sensor head consists of a miniaturized hollow cavity with a deflectable polymer diaphragm. The absorption of C_2H_2 within the cavity generates an acoustic pressure wave, which causes deflection of the diaphragm. The hollow cavity also acts as a Fabry-Pérot interferometer where the deflection of the diaphragm is detected with high sensitivity. The sensor has a good linear response in the range of 0.05−1.0% (v/v) and is capable of detecting 4.3 ppm of C_2H_2.

A FOCS for H_2S gas uses zinc oxide (ZnO) along with SPR detection via lossy mode resonance (LMR) as the readout technique.[76] Three sensor probes were fabricated by coating the unclad core with three different sensor films: The first consisted of a ZnO film and an over layer of ZnO nanoparticles, the second of a layer of ZnO nanoparticles, and the third of a silver film and a thin overlayer of ZnO. Their performances were compared, and the first sensor (coated with a ZnO film and an overlayer of ZnO nanoparticles) exhibited the highest sensitivity to H_2S. Another SPR-based sensor for H_2S was developed using a multilayer coating composed of a silver layer and a layer of indium tin oxide doped with nickel oxide.[77] Three kinds of probes for H_2S were fabricated. All have a first layer of silver on the unclad core of the fiber, but they differ with respect to their overlayers that consisted of either nickel oxide, or indium tin oxide, or indium tin oxide doped with nickel oxide. The resonance wavelengths shifts toward higher wavelength with increasing concentrations of gaseous H_2S near the probe. The effect is due to the interaction of H_2S with the sensing layer (silver is known to react with H_2S to form black Ag_2S), and this results in the change in its dielectric function. H_2S gas in the 10−100 ppm concentration range can be accurately and selectively determined. The largest shift is observed in case of using nickel oxide-doped indium tin oxide. The Gupta group[78,79] reported on a fiber-optic sensor for gaseous H_2S that was obtained by coating an unclad portion of a fiber with thin films of copper and zinc oxide via the thermal evaporation technique.[78,79] The exposure of the sensor to H_2S changes the dielectric function of zinc oxide, and a dip is observed in the transmitted spectrum. With increasing concentrations of H_2S, the resonance wavelength shifts to longer wavelengths, and this is exploited to sense the gas in the 0−100 ppm range. The typical response time and recovery time is about 1 min. Zhou et al.[80] describe the use of a silver-coated fiber Bragg grating (FBG) as a sensor for H_2S. The silver layer was coated on the cladding surrounding the surface of the FBG, and its exposure to H_2S gas changes the absorption spectrum. There is a linear relationship between the sensor signal and H_2S concentration in the range from 0 to 9.3%. However, the H_2S

DOI: 10.1021/acs.analchem.5b04298
Anal. Chem. 2016, 88, 203−227

gas interacts irreversibly with the silver coating. Such "sensors" can only be used once.

The group of Bond[81] has described a highly sensitive Raman detection of various gases and vapors (including nitrogen, oxygen, CO_2, toluene, acetone, and 1,1,1-trichloroethane) using a hollow core photonic crystal fiber probe. Sensitivity is enhanced by 3 orders of magnitude compared to direct detection. By combining Raman spectroscopy and photonic crystal fiber technology, a promising platform for gas sensing in environmental control was developed. Metal oxide nanoparticles such as those consisting of TiO_2, V_2O_5, or WO_3 were tested as coatings for constructing fiber-optic gas sensors.[82,83] However, the signal changes of these sensors remain weak, and both response times and recovery times are in the order of 1 h.

Ammonia. Ammonia (NH_3) is one of the major air pollutants emitted by the agricultural industry. Sources of ammonia include manure from animal feeding and fertilizer from cropping systems. Sensors with the capability of continuous monitoring of ammonia concentration in air are needed to qualify emissions from agricultural activities and evaluate human and animal health status, to study the chemistry of ammonia in context with environmental issues, and to provide baseline data for air quality standards. Sensing of both gaseous and dissolved NH_3 is of interest. A FOCS for gaseous NH_3 was developed by using tapered optical fibers coated with nanoassembled coating with a thickness of some 10 nm.[84] The coating is composed of tetrakis(4-sulfophenyl)porphine (TSPP) and poly(allylamine hydrochloride) (PAH), which was deposited on the fiber via an electrostatic self-assembly process. The exposure of the sensor to NH_3 induced changes in the transmission spectrum, and a linear response is found for the NH_3 concentration range from 10 to 100 ppm (v/v). The limit of detection is as low as 2 ppm, and the response time is less than 100 s.

By replacing the cladding of a two-layer poly(methyl methacrylate) fiber by a coating consisting of single-walled carbon nanotubes (SWCNT), an FOCS for NH_3, methanol, and ethanol vapors was obtained.[85] It can detect the three vapors in the 0−500 ppm concentration range at room temperature. The thickness of the SWCNT coating affects sensitivity in different ways: a thinner coating is good for sensing of NH_3, while a thicker one is beneficial for alcohol sensing. Aluminum oxide[86] and samarium oxide[87] annealed at 1200 °C can be used for sensing these three vapors as well. The cladding of an optical fiber was removed and coated with a thin film of aluminum oxide or samarium oxide. The RI of the cladding changes on exposure to these vapors and this, in turn, induces a change of evanescent wave absorption. The sensor typically covers the 0−500 ppm concentration range.

Carbon materials such as carbon nanotubes and graphene also found applications in sensors for NH_3. The group of Gupta[88] describes an SPR-based fiber-optic sensor for NH_3 that was fabricated by coating the unclad region of an optical fiber with a layer of copper, and an overlayer of a nanocomposite consisting of poly(methyl methacrylate) (PMMA) and reduced graphene oxide (rGO). The use of this nanocomposite enhanced sensitivity which is found to be higher than that of sensors made from PMMA or rGO coating alone. The sensor is capable of sensing NH_3 gas in the concentration range of 0−100 ppm with good selectivity over other gases including H_2S, Cl_2, H_2, and N_2. The combination of silver coating and an overlayer of rGO film on the unclad region of a fiber gave another optical sensor for NH_3. However, this sensor has slow reversibility,[89] and analytical ranges and response times were not given. Kavinkumar and Manivannan[90] deposited silver nanoparticles on exfoliated graphene oxide (GO) and found this coating to be sensitive to gaseous NH_3 in the 0−500 ppm concentration range. However, the response signal is also very small, and the sensitivity is strongly dependent on the concentration of silver nanoparticles on GO.

As had to be expected from earlier work, a bent optical fiber coated with sol−gel silica polymer doped with pH indicator bromocresol purple (BCP) was found[91] to be sensitive to NH_3. Its response is slowly reversible, and gaseous NH_3 can be detected at ppb (v/v) levels. This makes it suitable for monitoring trace concentrations of NH_3 in air of animal feeding facilities. Changes in air CO_2 concentration do not affect the sensor, but relative air humidity (RH) and temperature interfere. This undesired effect can be eliminated by acquiring calibration plots at different temperatures and RHs, but this obviously also requires temperature and RH to be sensed. A highly SPR-based FOCS for low concentrations of NH_3 gas was developed by using BCP.[92,93] It was obtained by coating an unclad core of the optical fiber with successive layers of indium tin oxide (ITO) and BCP. Absorption of NH_3 by the BCP layer is said to increase the RI, which further induces the resonance wavelength shift. The ITO layer also increases the resonance wavelength because it is porous and has grains. This allows the reaction products to enter the pores of the ITO layer and to cause swelling of the layer which is accompanied by an increase in the RI. The detection range is from 0 to 10 ppm, and the sensitivity is up to 1.9 nm/ppm with optimized thickness of the BCP layer. In addition, the sensor has a good selectivity over gases such as H_2S, CO_2, CH_4, H_2, Cl_2, and nitrogen. The well-known detection scheme for NH_3 based on the use of pH indicators placed in a gas-permeable matrix was refined by Rodríguez et al.[94] who describe a fiber-optic NH_3 sensor that utilizes a mixture of several pH indicators of various pK_a values. This sensor displays sensitivity to NH_3 over a wide range of wavelengths, and each spectral region has its characteristic response to NH_3 which allows ratiometric and, therefore, more robust sensing. The pH indicators were incorporated into a hydrophobic and well NH_3-permeable film of polyurethane and then deposited on the unclad region of an optical fiber. The sensors works in the NH_3 concentration range from 0 to 100 ppm.

Not unexpectedly in view of earlier respective work, the color of certain new cobalt−organic ligand complexes was found to be sensitive to NH_3 gas.[95] Ammonia can exchange the organic ligand, and this induces changes in visible-near-infrared absorption. The cladding of a multimode-fiber was removed and coated with the cobalt complex to give an FOCS for ammonia. It was found that the length of aliphatic side chains in the organic ligand strongly affect the sensitivity, with the lipophilic ligand exhibiting better sensitivity. Another optical fiber sensor for ammonia uses a tapered multimode fiber coated with polyaniline nanofibers.[96] The optical properties of polyaniline have been long known for being pH dependent. After exposure to NH_3, the absorption of the evanescent field changes. Sensitivity can be adjusted via the diameter of the tapered fiber and is highest when the diameter is reduced to 20 μm. It takes less than 3 min to measure a sample, but it takes almost 10 min until full recovery.

Ethanol. Sensors for real-time monitoring of ethanol (in the gas phase and in fluids) have a wide application that range from

DOI: 10.1021/acs.analchem.5b04298
Anal. Chem. 2016, 88, 203−227

testing for drunk drivers to analysis of hard liquors and fuel. Given the fact that fiber-optic sensors have compact size and low power consumption, they are attractive with respect to the design of hand-held devices for on-site detection of alcohol. A coating composed of SnO_2 and SnO_2/CuO nanoparticles was found to show ethanol-sensitive absorption[97] in that absorbance decreases with increasing concentration of ethanol vapor. Compared to an SnO_2 nanoparticle coating, the use of SnO_2/CuO results in 3-fold improved sensitivity. The sensor can quantify ethanol vapor in the range from 0 to 500 ppm. An extended analytical range (from 1000 to 20 000 ppm) was reported for an evanescent fiber-optic ethanol sensor based on the use of amorphous SnO_2 nanoparticles.[98] Similar to the SnO_2 and SnO_2/CuO, other kinds of inorganic nanoparticles were tested. These are made from $Li_2B_4O_7$ that was doped with Co and Cu,[99] or Gd-doped ZnO nanoparticles,[100] or both undoped and Mn-doped Co_3O_4 nanorods.[101] These also can detect ethanol via a decrease in their absorbance on exposure to alcohol vapor. In the case of Co_3O_4 nanorods, the undoped nanorods exhibit even higher sensitivity than the Mn-doped Co_3O_4 nanorods.[101]

Organic materials such as carbon nanotubes (CNTs) were also employed as sensing materials for ethanol.[102,103] A multimode optical fiber tip was coated with CNTs by a drop-casting technique and annealed at 70 °C. The reflectance of the sensor decreases with increasing concentration of ethanol in the range from 5% to 80% (v/v) in water. If the CNTs are treated with iso-butyl methyl ketone, sensor performance is further improved in giving a 2- to 3.4-fold increase in sensitivity for both methanol and ethanol.[104] However, all the above sensors display a rather small signal change.

Sensitivity is improved if tapered fibers are used.[105] Such sensors are based on the measurement of RI of water−ethanol mixtures. By decreasing the taper ratio and increasing the length of the taper, the sensitivity is as good as 1.527 mV/%, and the sensor can detect changes in the concentration of ethanol in water as small as 0.655%. Tapered optical fibers also were coated with a nanocomposite consisting of silver nanoparticles and rGO and was used for sensing ethanol in aqueous solutions.[106] The absorbance of the nanocomposite on the fiber decreases with increasing amount of ethanol, and response is linear in the 1−100% concentration range.

Porous silicon was applied in a sensor for vapor detection.[107] Manufacture involves hole milling of the fiber socket, fabrication of filter structure, and integration of the fiber-optic cable to the silica bulk. Reflectivity changes on exposure to alcohols. It was stated, though, that this sensor necessitates a thorough fabrication process. The finding that the fluorescence intensity of silicon quantum dots increases if the dots are exposed to vapors of water and alcohol resulted in the design of an optical fiber sensor with silicon quantum dots placed at the distal end of the waveguide.[108] The sensor has a fast and reversible response but has to be recovered by subsequent exposure to dry (and preferably hot) gaseous oxygen, but on the other side, it did not degrade even after 30 sensing cycles.

Other Volatile Organic Compounds (VOC)s. VOCs have been detected[109] with a device where the cladding of an optical fiber was replaced by a film doped with the organometallic compound $[Au_2Ag_2(C_6F_5)_4(C_6H_5C{\equiv}CC_6H_5)_2]_n$. This compound is negatively charged and can be deposited on the fiber cladding by means of the layer-by-layer technique using a positively charged polymer. The thickness of the sensing film is in the nanometer range, and lossy-mode resonances (LMRs) can be induced. When exposed to alcohol vapor, reversible LMRs shifts are induced whose magnitude can be related to the concentration of vapors of ethanol, methanol, or isopropanol. The sensor is highly sensitive. In the case of methanol, the LMR peak is blue-shifted by almost 100 nm. RH of <60% and temperature in the range of 20−60 °C do not adversely affect response.

A single-headed polymer optical fiber sensor array was described for sensing VOCs using hydrophilic GO and hydrophobic rGO.[110] The principle of operation of sensor transduction relies on the dependence of the reflectance on the optical and geometric properties of the sensing layers when vapor molecules are adsorbed on the GO and rGO layers. The arrays can distinguish between tetrahydrofuran and dichloromethane, even in the presence of 90% RH. VOCs can also be determined via Rayleigh scattering using a hollow-core photonic crystal fiber (HC-PCF).[111] The VOCs enter the air holes of the HC-PCF so that the Rayleigh scattering is induced which is accompanied by an intensity loss of transmitted light. The optical output was measured with a power meter, and the sensitivity was ∼0.022 dB/ppm for sensing ethanol vapor.

The distal end of an optical fiber was coated with a film of porous silica xerogel in order to sense VOCs in the reflection mode.[112] Silanol groups on the xerogel act as weak acids and interact strongly with molecules that contain hydroxy groups like alcohols, π-electrons like toluene, or a lone pair of electrons like acetone. The adsorption of VOCs on the xerogel causes a change in the reflected optical power so that concentrations of VOCs can be quantified. A wide range of compounds including 2-propanol, toluene, 1-butylamine, acetone, cyclohexane, and ethanol was investigated, and the sensitivities vary according to the compound. Methanol and ethanol are so strongly adsorbed on the sensing film that adsorption is irreversible.

Another kind of FOCS for VOCs is making use of a very thin film of the solvatochromic dye Nile red.[113] The respective setup is shown in Figure 2. A section of the fiber cladding was polished and coated with a layer of Nile red. On exposure to different VOCs, the absorption spectra of Nile red are shifted, and a heterodyne frequency modulation method was used to quantify the spectral changes. The time period of the modulated sensing signal linearly shifted with the concentration of the VOCs. Dimethylamine, ethanol, benzene, acetic acid, and toluene can be accurately sensed in the 0−5 ppm concentration range. The response time typically is 35 s. Several other solvatochromic dyes were also investigated.[114] All these sensors display different sensitivity, and principal component analysis may be used to distinguish between VOCs. Fiber-optic pulse width modulation was applied in a sensor for low concentration VOC gases.[115] By incorporating Nile red and poly(vinylpyrrolidone) (PVP), a sensing membrane coating was fabricated on a side-polished single-mode fiber. This coating utilized Nile red's solvatochromic properties of changing optical characteristics upon VOC absorption. The sensing membrane coating produced strong signals that were fast and reversible when exposed to VOC gases such as benzene. An oscilloscope and an optical spectrum analyzer were used to analyze the performance of the sensor device. The PWM sensing system was tested for the resonance wavelength shift induced by varying concentrations of benzene vapor and was found to be superior to other analyzers and sensors. Sensitivity to the benzene vapor was 7.79 ns/ppb with highly reproducible response and recovery times of less than 50 s.

DOI: 10.1021/acs.analchem.5b04298
Anal. Chem. 2016, 88, 203−227

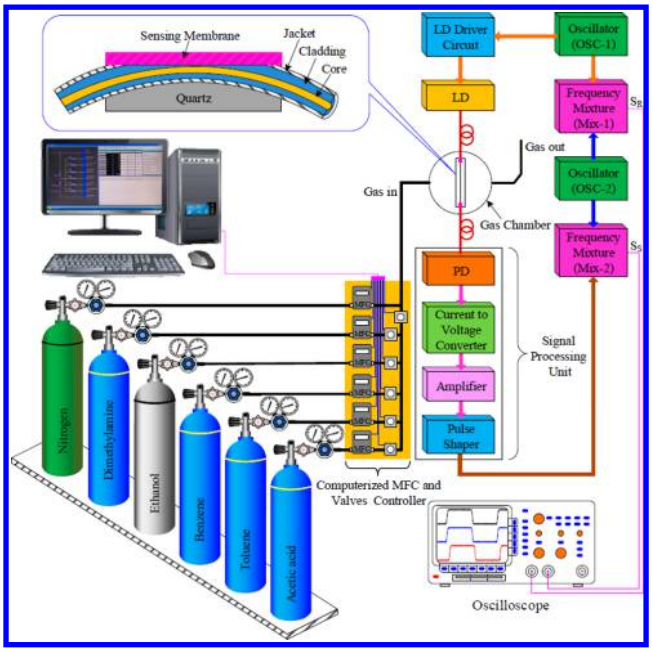

Figure 2. Schematic of the experimental setup of the heterodyne frequency modulation VOC sensing system. (Reproduced with permission from Khan, M. R. R.; Kang, S.-W. *Sensors* **2014**, *14*, 23321 (ref 113). Copyright 2014, MDPI AG, Basel, Switzerland.)

The porphyrin tretraphenylporphyrinsulfonate (TPPS) can quickly switch between different aggregation states (of the J- and H-type) in response to the presence of acidic or basic vapors. These forms display distinct spectral features. This phenomenon has been explored in a detector for acidic vapors.[116] The core region of a fiber end was coated with a film of TPPS via a self-aligning UV-induced procedure to produce a fiber-optic sensor. It has to be activated with ammonia vapor first and then is contacted with acidic vapors. A sharp resonant light scattering signal at 490 nm was emerged that was used to detecting hazardous acidic gases. The sensor exhibits good stability over 8 detection cycles. However, it needs to be regenerated in ammonia after each use. Cheng and co-workers[117] make use of fluorescent conjugated polymer doped with Pd(II) tetraphenylporphyrin (PdTPP) as a highly sensitive material for detecting vapors of organic amines. PdTPP was doped in the fluorescent polymer polyfluorene (PFO) such that PdTPP quenches the fluorescence of PFO via electron/energy transfer. Once the electron-donating organic amine binds to PdTPP, the electron/energy-transfer process is suppressed and fluorescence is recovered. This results in a lasing turn-on action under optical pump and in a more than 5-fold improved sensitivity compared to methods based on spontaneous emission. Various vapors of organic amines were detected in <1 min. It should be kept in mind, though, that PdTPP is a highly sensitive luminescent probe for oxygen.

A FOCS for measuring acetone, isopropanol, and benzene was developed using TiO_2 nanomaterials to modify the cladding region of a fiber.[118] The exposure of the sensor to these vapors causes the changes in RI of the cladding and induces changes of evanescent wave absorption. The peak absorption intensity of the sensor changes linearly with the increasing concentration of the vapors, and nanomaterials annealed at different temperatures play an important role in the sensitivity. However, the changes of absorption intensity are too small for practical use. A fiber-optic probe of about 200 μm in diameter was applied in a surface enhanced Raman spectroscopic (SERS) sensor that uses poly(methyl methacrylate) monoliths functionalized with silver nanoparticle in a capillary.[119] It enables trace determination of pesticides such as phosmet. The SERS enhancement factor is approximately 1.2×10^8; the detection limit is 3 $\mu g \cdot L^{-1}$, and response is linear in the 3−1000 $\mu g \cdot L^{-1}$ concentration range.

SENSORS FOR HUMIDITY, WATER FRACTIONS, HYDROGEN PEROXIDE, AND HYDRAZINE

Humidity. Optical humidity sensors have numerous applications, examples being the chemical industry, aviation, climate research, and food technology. The typical volume fraction of water in the lower atmosphere is approximately 1.2%. Even traces of water in the industrial gases can cause serious quality problems in the production of semiconductors. Therefore, it is important to monitor and to control trace water levels in industrial gases at each supplying step and especially during their use. Numerous materials are known for changing color or density on exposure to water vapor, the challenge being a response over a wide range of RHs, achieving a large signal change and full reversibility, and making sensors insensitive to air pollutants and temperature. An FBG sensor was built using a polyimide coating for measuring RH.[120−122] The polyimide coating exhibits peculiar swelling properties, which induces the tensioning of the coated grating and subsequent signaling of the change in RH through a shift of the Bragg peak wavelength. A resolution of 2% RH (which is moderate) was achieved, and the response range is between 25% and 65% of RH. Most hydrogels also absorb moisture well and can be used for constructing RH sensors. An intensity-based fiber-optic RH sensor was formed by solidifying mini-hydrogel spheres on bare fiber cores.[123] RH changes the RI of hydrogel spheres and thereby causes the intensity of the light transmitted through the fiber to change. The size and number of the spheres play big roles in sensor performance. Bigger and more spheres on the fiber core result in higher sensitivity, but the analytical range is narrower (70% to 90% RH).

RH can also be determined with a fiber-optic sensor based on variation in the resonance frequency of a mechanical silicon microstructure that has a silica gel granule mounted on it.[124] Again, the absorption of moisture on the gel changes the resonance frequency, and the mass of absorbed moisture is linearly dependent on the RH of air. The sensor is capable of measuring RH in the range of 0−100%. A side-illuminated optical fiber sensor for RH was designed by replacing the cladding of a fiber by poly(vinyl acetate) doped with the polarity-sensitive indicator probe called Reichardt's dye or ET30.[125] The device uses leaky modes as the signal carrier, and the signal increases linearly with increasing RH. The complete range of RH can be accurately determined, resolutions being between 0.11% and 0.25%.

An optical fiber RH sensor without a hygroscopic coating was described that measures the near-infrared absorption of water vapor at around 1368 nm.[126] An air-guided photonic crystal fiber in a semiconductor optical amplifier was employed as the sensor head, and the amplifier acts as the gain medium in a ring laser. The voltage difference between zero absorption baseline and absorption signal at the water absorption peak was used to determine RH. The sensor can operate in the 0 to 90% RH range with good linearity and a sensitivity of up to 10.9 mV per 1% of RH.

DOI: 10.1021/acs.analchem.5b04298
Anal. Chem. 2016, 88, 203−227

An evanescent wave sensor for RH was prepared from an electrospun nanofiber coated with poly(acrylic acid).[127] The diameter of fiber and the mat density play important roles in determining the sensitivity. Higher sensitivity is accomplished by using lower diameter nanofibers (if not tapered fibers) and higher mat density. The sensor operates in the 30−95% RH range and responds within a minute, while the recovery time is only 210 ms. Similarly, a tapered plastic optical fiber, if coated with agarose gel, or a hydroxyethylcellulose−polyvinylidene-fluoride composite, or a nanostructured ZnO film can sense RH.[128] The RI of the coating changes as it swells after absorption of water. The three sensors have good sensitivity in the 50−85% RH range, and the one based on a ZnO nanostructure has the highest sensitivity. The sensitivity can be further improved by doping the ZnO with aluminum.[129]

A Fresnel reflection-based optical fiber sensor with an array-waveguide grating (AWG) was coated with poly(vinyl alcohol) (PVA) and used for multipoint RH measurement.[130] Every channel end of the AWG was split to form a vertically planar surface and then coated with a layer of PVA whose RI is sensitive to moisture. The changes in the RI strongly affect the Fresnel reflection, and the measurement of reflection intensity of each channel allows for multiple sensing of RH. More than 15 samples can be measured simultaneously with such a sensor array, and the analytical range is 30−80% RH.

The PVA coating was also applied in another sensing scheme that is based on a photonic crystal fiber with an in-fiber Mach−Zehnder interferometer and an FBG for simultaneously measuring RH and temperature.[131] The resolution can be as good as 0.13% RH in the 30−95% range, and temperature can be resolved by up to 1.0 °C. Such dual sensors are particularly attractive because they can automatically correct for effects of temperature which are quite large in such sensors. Another dual sensor for RH and temperature is using sensing elements with multilayer coatings consisting of nanoporous TiO_2 and SiO_2 placed at the distal fiber end.[132] RH changes the effective RI of the coating, and this induces a shift of the interference fringe pattern of a Fabry-Pérot structure. The sensor has a good repeatability and is particularly sensitive at low moistures (1.8−75% RH). Temperature can be measured in the range from 21.4 to 38.8 °C. Grattan and co-workers[133] designed a Michelson interferometer-type sensor probe by coating the distal end of a long-period grating (LPG) with a silver mirror to form an LPG grating pair. This technique overcomes the limitations of earlier LPG-based sensors which had difficulties in detecting the broad bandwidth of the attenuation bands formed by the propagation mode coupling between the core and the cladding modes. The sensor was further coated with PVA to give an FOCS for measuring RH. The PVA coating swells with increasing humidity and thereby causes changes in the RI of the probe. This sensor configuration also enables shifts in the attenuation of bands to be more easily detectable. Due to its good resolution, RHs in the range from 20% to 85% can be precisely determined. By depositing a hydrophilic agarose gel on a tapered plastic optical fiber, another kind of optical fiber sensor for RH was constructed.[134] Agarose reversibly binds and releases moisture, and this alters its refractive index which, in turn, changes the intensity of light propagating in the fiber. RH can be sensed in the range from 50% to 80%. Such sensors can be produced at low cost and provide an economical and flexible approach for measuring RH. Another sensor for RH is making use of reduced graphene oxide,[135] but it only works in the 75% to 95% RH range.

A high performance FOCS for measuring RH (referred to as "water content") in industry gas was designed using copper benzene-1,3,5-tricarboxylate (Cu-BTC) metal organic framework (MOF) as sensing material (Figure 3).[136] The color

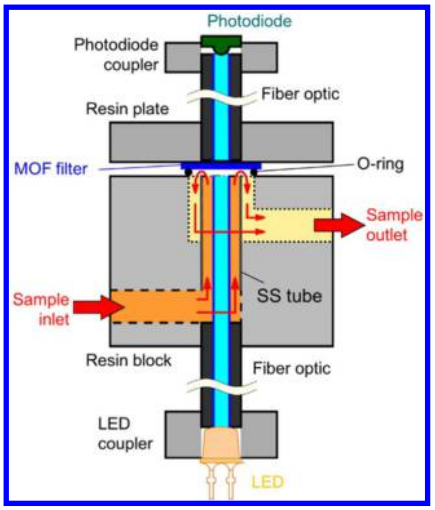

Figure 3. Schematic of a fiber-optic humidity sensing device based on the use of a metal−organic framework (MOF) of the type Cu-BTC-MOF (see text). The color of the MOF filter changes when absorbing water molecules and further induces changes in absorbance. This serves as the analytical information for sensing water vapor. (Reprinted from *Anal. Chim. Acta*, Vol *886*, Ohira, S.-I.; Miki, Y.; Matsuzaki, T.; Nakamura, N.; Sato, Y.-k.; Hirose, Y.; Toda, K. A fiber-optic sensor with a metal organic framework as a sensing material for trace levels of water in industrial gases, pp. 188−193 (ref 136). Copyright 2015, with the permission from Elsevier).

depth and tone of Cu-BTC changes with water adsorption, an effect long known for simple salts of copper(II) and cobalt(II) but not yet reported for MOFs. Cu-BTC crystals appear deep blue in dry gases but change to light blue in wet gases. The sensor shows a reversible response to trace water in gas, and heating is not required for removal of the adsorbed water molecules. Sample flow rate did not influence the sensitivity, and the detection limit is up to 40 ppbv. It takes only 23 s to measure a sample. The standard deviation for daily analysis of 1.0 ppmv H_2O standard gas over 20 days was only 9%. More importantly, the sensitivity of the sensor is not dependent on the type of industry gas, which make it suitable for measuring trace water in different industry gases. The performance of a known FOCS for RH water vapor in natural gas in the presence of methanol and ethylene glycol was compared to several kinds of hygrometers.[137−139] The RH sensors included those based on (a) capacitive detection, (b) a quartz crystal microbalance, (c) an electrolytic cell, and (d) a chemical volumetric detection by conversion of water to acetylene with the reagent calcium carbide.

Water Fractions in Organic Solvents. Sensing the fraction of water in industrial solvents is critical not only to quality control and for safety reasons but also because water inhibits certain large-scale chemical reactions such as the Grignard reactions. A fiber-optic quasi-distributed sensor was developed for detecting the location and severity of water leakage.[140] A vessel of water absorbing material called water combination soil (WCS) is deposited between two highly reflected connectors. One acts as a reference, the other as the sensing connector. The absorption of water causes the WCS to

DOI: 10.1021/acs.analchem.5b04298
Anal. Chem. 2016, 88, 203−227

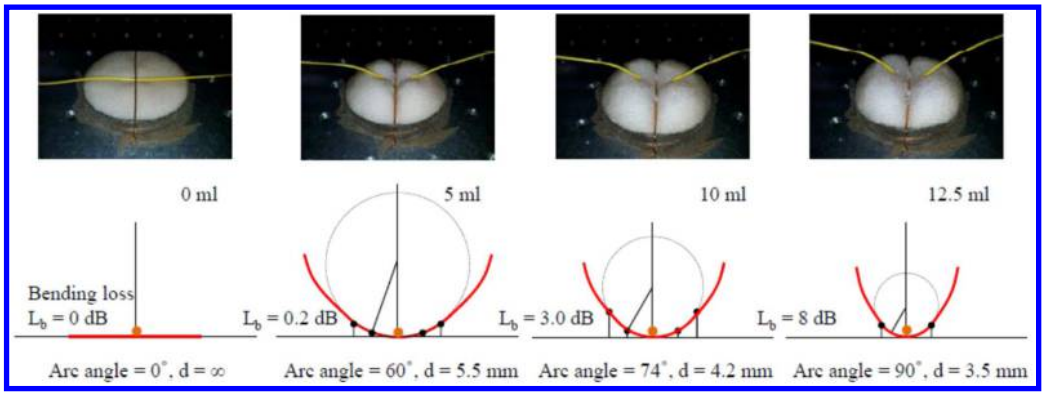

Figure 4. Bending loss according to bending diameters and arc angles of an optical fiber. (Reproduced with permission from Cho, T.-S.; Choi, K.-S.; Seo, D.-C.; Kwon, I.-B.; Lee, J.-R. *Sensors* **2012**, *12*, 10906 (ref 140). Copyright 2012, MDPI AG, Basel, Switzerland.)

expand, and this induces a bending loss in the optical fiber (Figure 4). The effects of vessel size of the probes on sensitivity were studied, and the results showed the larger vessel probe to be more sensitive.

The fraction of water (H_2O) in deuterium oxide (D_2O) can be quantified with an evanescent wave fiber sensor[141,142] that is based on absorption spectroscopy in the IR (typically at 2.9 μm). A least-squares model is utilized for building the calibration model and to calculate the water fraction. Low levels (0−2.5%) of H_2O in D_2O can be measured accurately. The same sensing system was used to measure the water fraction in hydroxylic organic solvents such as glycerol, ethanol, and glycol at an absorption wavelength of 2.7 μm.[143] Photonic crystal-based sensors for organic solvents and for solvent−water mixtures were described.[144] The fluorescence of an europium chelate was found to sensitively respond to water fractions in organics, and a respective luminescence lifetime-based FOCS was designed.[145] A polymerizable europium(III) complex was photocopolymerized into an acrylamide-*co*-methacrylate matrix on a silanized glass slide to yield a so-called "optode" (optical sensor) membrane. The time-gated luminescence intensity and decay time of the europium chelate decrease with increasing fractions of water in the (organic) solvent. The analytical ranges depend on the solvent, and the largest ranges were found for ethanol and acetonitrile (0.20−10.0%). This sensor is well reproducible, reversible, and fast.

Hydrogen Peroxide. H_2O_2 is an important industrial chemical but also produced by enzymes out of the group of oxidases. FOCS for H_2O_2 are almost exclusively based on the oxidation-capability of H_2O_2, which generate the analytical signal after the oxidation reaction. Because of this sensing principle, all these "sensors" suffer from irreversible response. Silver nanoparticles have been used for constructing an FOCS for H_2O_2.[146,147] The sensor utilized a combination of SPR and localized SPR for detection and operated in wavelength interrogation mode. The optical fiber core is first coated with a silver layer and further overcoated with a poly(vinyl alcohol) polymer containing silver nanoparticles (AgNPs). The resonance wavelength shifts over the 10^{-8} to 0.1 M concentration range. Response is due to the catalytic decomposition of H_2O_2 by AgNPs. This results in the degradation of the NPs which changes the RI of the nanocomposite layer and causes the shift in resonance wavelength.

Another kind of FOCS for H_2O_2 was fabricated by immobilizing Prussian white within a multilayer of electrostatically self-assembled polyelectrolytes on fiber head.[148] When Prussian white is oxidized back to the blue state due to the presence of H_2O_2, the intensity of the reflected light will change concomitantly. The temperature influences on the sensing performance is systematically studied, and the amplitude of the intensity of reflected light is found to vary with temperature. However, the detection range and detection limit are not characterized.

■ SENSORS FOR pH VALUES, IONS, AND SALINITY

Optical sensing of pH remains to be of wide interest even though all optical sensors suffer from cross sensitivity to ionic strength. The number of articles on pH sensors is decreasing, though, which does not come as a surprise in view of the state of the art and the fact that FOCS for pH are commercially available. On the other hand, the response of optical pH sensors covers a limited range of pH only (in most cases), typically 3 pH units. It also needs be stated that many pH sensors presented in the past few years are (minor) modifications only of previously reported sensing schemes and materials and that authors often do not properly cite previous work on the subject. In the worst case, sensors are presented that are inferior to others described before. Such sensors are not treated here. One notes a need for sensors covering the extremes of pH values (<1 and <12) and having operational lifetimes of >1 day. This still appears to represent a substantial challenge in terms of material sciences.

pH Values. The pH value is by far the most often measured chemical parameter in industry, research, medical diagnosis, and daily life. Fiber sensors for pH are commercially available but not perfect. Recently, an SPR-based FOCS for pH was prepared by coating an unclad core of an optical fiber with three consecutive layers of silver, silicon, and a pH-sensitive hydrogel.[149] The pH change in the fluid causes the swelling or shrinkage of the hydrogel layer, and this changes its RI. An increase in the pH of the solution induces a blue shift (ΔS) of the resonance wavelength, and the sensor is capable of measuring pH values between 3 and 12 which is a wide range indeed. However, the sensitivity (ΔS/pH) at neutral pH values is relative small, and the device therefore can resolve pH values of not more than ±0.1 units at best, but this is adequate when measuring pH under harsh conditions. The corrugated long period fiber grating element is highly sensitive to RI. By coating it with a pH-sensitive material [poly(vinyl alcohol) and poly(acrylic acid); PVA−PAA], a fiber-optic pH sensor is obtained that can detect pH's in the range of 3−6 with a

DOI: 10.1021/acs.analchem.5b04298
Anal. Chem. 2016, 88, 203−227

resolution of 0.02 pH units.[150] The same PVA−PAA coating was applied to develop an interferometric pH sensor.[151]

By integrating the fiber-optical sensing technique with wireless data transmitting technology, a hybrid wireless sensor network was established.[152] The optical sensors were obtained by covalent immobilization of two coumarin-based pH-sensitive fluorescent probes on the fiber head, and pH's can be measured in the range from 1 to 9. The sensor network can sense pH over a large area, and data can be wirelessly and remotely collected at a base station.

An adsorption-based evanescent wave FOCS was constructed by immobilizing the pH sensitive indicator bromophenol blue in an ormosil hybrid material.[153] The sensor can reversibly determine pH's in the range from 3 to 9, but precision is poor (0.2 pH units). Intended for use in on-body monitoring pH's in biological fluids, it will not meet current stipulations at present, however. No degradation of the sensing fiber was found over 24 h of continuous measurement. The use of a combination of indicators in order to measure a wider range of pH's was reinvented.[154] The indicators phenol red, cresol red, and phenolphthalein were incorporated into a mesoporous sol−gel host material which then was placed on an uncladed plastic optical fiber. The sensor can measure pH in the range from 3 to 11. The effects of film thickness, RI, and porosity on sensor performance were studied, but unfortunately, the resolution of the sensor is not specified.

An unusual fiber-optic pH sensor was developed that is based on a composite prepared from plasmonic gold nanoparticles, palladium nanoparticles, and rhodamine B.[155] Seemingly a pH insensitive material, their incorporation into silica will render it pH-sensitive because the transmission varies with the surface charge density which depends on pH. The response of this sensor to pH is rapid, reversible, and sensitive in the range from pH 2 to 10. The charming aspect of this work is its wide scope in that numerous kinds of materials may be used for pH sensing, and, possibly, also for other sensors if one can govern surface charge. Zhao et al.[156] have used another kind of charge-sensitive material in order to sense pH values. Nanoporous poly(ionic liquid) membranes with hierarchical and unique pore architectures were prepared via electrostatic complexation between imidazolium-based poly(ionic liquid)s and poly(acrylic acid) in a variety of morphologies. Coating the membrane onto the surface of an optical fiber resulted in a device with high pH-sensing performance in terms of the response rate and the sensitivity, due to the charge and porous nature of the membrane layer.

Time-of-flight fluorescence detection enables spatially resolved determination of pH values, for example, along the length of an optical fiber. A respective sensor was constructed[157] by covalent attachment of a fluorescein derivative onto a highly porous poly(ethylene glycol diacrylate) support and then attached to the distal end of an optical fiber. Fluorescence was read out by both time-correlated single photon counting and stroboscopic detection. The resolution of the sensor is 0.02 pH units which is quite good. However, the detection of such short (nanosecond) lifetimes requires rather sophisticated electronics, and spatial resolutions are inferior to sensors where longer-lived pH probes are used. The same group later used the same material to build an evanescent-wave-based sensor for pH. It covers pH's in the 5−9 range with an accuracy of 0.08 pH units at pH 7.[158] Another fluorescein-based pH sensor was obtained by coating a tapered spherical probe head with an ormosil film covalently doped with the indicator dye.[159] Features include high stability and good pH sensing ability, a resolution of 0.05 pH units in the biologically meaningful pH range of 6.1−7.8, a tip size of only 70 μm, and the possibility of performing measurements at a single-cell level.

Ions. Metal ions are commonly sensed optically via chelation with organic chromophores or fluorophores. For example, a fluorescence lifetime-based sensor for sodium ion uses a 1,2,3-triazole fluoroionophore as the recognition/transduction element.[160] Chelation of sodium ion by the probe enhances its fluorescence intensity and decay time (in the ns time regime). The sensor works in the 1−20 mM concentration range and has acceptable accuracy. In another kind of FOCS for Zn^{2+} ion,[161] the cladding of an FBG was coated with a perylene monoimide dye. Chelation with Zn^{2+} ion changes the RI of the coating, and this can be applied for highly selective FBG sensing of Zn^{2+}. The sensor can be reused after treating it with a solution of EDTA which strips off Zn^{2+}. Unfortunately, the sensor was tested for its response to 1.0 M Zn^{2+} ion solution only, and response time and detection range are not provided.

A surface enhanced Raman scattering (SERS)-based optrode for Cd^{2+} was described[162] where the tip of an optical fiber was self-assembled (layer-by-layer) with silver nanoparticles, followed by modification with a cadmium-chelating thiolated terpyridine. Following thiol-silver interaction, Cd^{2+} is chelated by the terpyridine which causes the SERS spectra to change. Response to Cd^{2+} is linear in the 10−200 μM concentration range which is fair. The sensor can be regenerated by treatment with EDTA. A dually responding sensor for both Cu^{2+} and Zn^{2+} was described that was obtained by replacing a fiber cladding with a layer doped with the fluorescent probes FluoZin-1 and dansyl.[163] Chelation with Zn^{2+} causes an enhancement of fluorescence, while Cu^{2+} ions quench fluorescence. This can be used to quantify the two ions. The dual sensor array can sense Cu^{2+} in the range of 0−3.0 mg/L and that of Zn^{2+} between 0 and 2.0 mg/L.

Heavy metal ions (HMIs) often exert a quenching effect on the fluorescence of organic and inorganic dyes and on many nanoparticles. This was exploited, for example, in a sensing scheme where monodispersed CdSe/ZnS Q-dots were encapsulated in a silica shell and then placed at the tip of an optical fiber in a PVA coating to obtain an FOCS for Cu^{2+}.[164] The luminescence intensity of the Q-dots decreases on interaction with Cu^{2+}, and normalized fluorescence intensity (I_0/I) is linearly related to the concentration of Cu^{2+} in the range from 0 to 10 μM. The resolution of the sensor is 0.9 μM, but response is irreversible.

A photonic crystal fiber (PCF) sensor was constructed for directly measuring the concentration of potassium chloride.[165] The PCF has circular air holes with diameter of 400 nm. The transmitted field emerging from the PCF varies linearly with the concentration of KCl, and this was used to detect high KCl concentrations (range: 2.5−20%). Photonic crystals were also applied to sensing and imaging of potassium ions by using a sandwich assembly composed of layers of photonic crystals and an ion-selective membrane.[166] The latter consists of plasticized poly(vinyl chloride) doped with the K^+-selective ion carrier valinomycin. The film has a red color if immersed into plain water, but green in 5 mM KCl and purple at KCl concentrations of 100 mM or higher. This 3D photonic crystal sensor responds to K^+ ions in the 1 to 50 mM concentration range (which covers the concentration range encountered in blood) and shows high selectivity over ammonium and sodium

DOI: 10.1021/acs.analchem.5b04298
Anal. Chem. 2016, 88, 203−227

ions. Sensor films were also imaged with a digital camera by exploiting the RGB technique.

An SPR-based FOCS for manganese(II) ion was obtained by coating an unclad fiber core with a nanocomposite with a layer of silver and then a film composed of polypyrrole and ZnO.[167] The interaction of Mn^{2+} with the sensing surface changes its dielectric constant and induces a red shift of the SPR spectrum. The sensor works in the 0−150 μg/L concentration range. Sensitivity strongly depends on the fraction of polypyrrole in the nanocomposite. Another pyrrole-based coating (in a composite with chitosan) was placed on a layer of silver metal and a layer of indium tin oxide, all on an unclad fiber core, and this multiplayer approach resulted in an optical sensor for the heavy metal ions Cd^{2+}, Pb^{2+}, and Hg^{2+}.[168] Again, the shift of the maximum of SPR forms the analytical signal, and Cd^{2+} can be detected with the lowest LOD (10 μg/L).

While not being a fiber-optic waveguide sensor, it is interesting to note that fiber-like materials also can be used as supports in sensors for visual inspection. Polyacrylonitrile fibers were modified with carboxymethyl−dithiocarbamate, and this material (see Figure 5) exhibits excellent selectivity and sensitivity for silver(I).[169] It changes its color from pink to red-brown in <10 s. The assay is selective, and the visual detection limit is 5.5 pM in the pH 2−12 range.

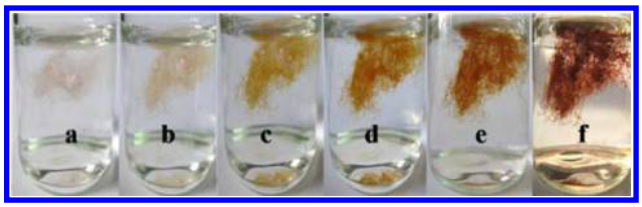

Figure 5. Response time of a carboxymethyl−dithiocarbamate modified polyacrylonitrile fiber for Ag^{+} (1×10^{-2} mol/L) at (a) 0 s, (b) 10 s, (c) 2 min, (d) 10 min, (e) 1 h, and (f) 24 h at pH 5.5. (Reprinted from *J. Hazard. Mater.* Vol. 297, Xing, X.; Yang, H.; Tao, M.; Zhang, W. An overwhelmingly selective colorimetric sensor for Ag(I) using a simple modified polyacrylonitrile fiber, pp. 207−216 (ref 169). Copyright 2015, with permission from Elsevier).

Mercury(II) ion remains to be a priority environmental and food analyte for obvious reasons. The group of Pollard[170] describes an evanescent wave-based FOCS for Hg^{2+} that uses the well-known chromogenic ligand dithizone which binds Hg^{2+} with good selectivity to form an orange colored complex with an absorption peak at ∼480 nm. The sensor covers the 0.1−5.0 ppm concentration range, and the detection limit is as low as 5 ppb. A porphyrin-functionalized polyacrylonitrile fiber similar to the one shown in Figure 5 exhibits excellent selectivity and sensitivity toward Hg^{2+} ion sensing.[171] Upon binding of Hg^{2+}, the color changes from red-brown to dark-green. Both absorption and fluorescence spectra change, and visual readout is possible. The limit of detection (20 ppb) is well below most allowed limits. The sensor material can be regenerated by treatment with dilute hydrochloric acid, and it was reused more than 50 times. Another fiber-optic-based evanescent wave sensor was developed for sensing elemental mercury utilizing gold nanorods.[172] Mercury adsorbs on the nanoparticles and causes a shift in the longitudinal localized SPR. The nanorods were deposited on the surface of a bare and strongly bent fiber-optic cable in order to excite the resonance and to determine the absorbance through the evanescent wave at the surface. There is a linear relationship between the SPR shift and mercury concentration in the range from 0 to 75 $\mu g/m^3$. Concentrations down to 1.0 $\mu g/m^3$ are detectable.

A fluorescence enhancement-based sensor for lead(II) (the most ubiquitous toxic metal ion in the world) is based[173] on the suppression of photoinduced electron transfer quenching in a dye referred to as SMPrb. If Pb^{2+} ion binds to the dye, electron transfer is hindered and fluorescence is restored. Fluorescence increases with the concentration of Pb^{2+} in the 4−200 μM concentration range, and the lower limit of detection is 126 ng/mL which is not sensational. A more sensitive fiber sensor for Pb^{2+} was described that exploits a DNAzyme.[174] The presence of Pb^{2+} ion cleaves the DNAzymes and releases fluorescently labeled fragments, which further hybridize with the complementary strands immobilized on the optic fiber sensor surface. Fluorescence intensity is measured with a portable device, and Pb^{2+} can be quantified in the 2−75 nM concentration range, with a 1 nM detection limit. The sensor has a very good selectivity over other heavy metal ions. The sensor also can be regenerated with a 1% solution of SDS of pH 1.9, and it was reused over 100 times without compromising sensor performance.

Fiber-optical sensing of anions is less common. Chemically tapered multimode optical fiber probes for fluoride were reported by Venkataraj et al.[175] They are based on quenching of the fluorescence of the natural dye curcumin and have a detection range that extends from 2 to 200 μM. The performance of the tapered probe was evaluated with respect to the probes that consist of combinations of bare uncladded multimode optical fibers. A review on methods for analyzing fluoride has appeared.[176]

Chromate is an analytical evergreen in terms of sensing. Often referred to as Cr(VI), it is of course an anion. Most earlier sensors rely on (a) the intrinsic yellow color of chromate or (b) its oxidative power that can lead, for example, to the (irreversible) formation of a dye. In a very different and reversible SPR-based sensing scheme,[177] the unclad core of an optical fiber was consecutively coated with layers of silver, indium−tin oxide, and the swellable hydrogel (3-acrylamidopropyl)-trimethylammonium chloride ($ATAC^{+}$). The sensor relies on the shrinkage/swelling of the hydrogel layer when exposed to chromate anion which is due to the formation of an ion pair between $ATAC^{+}$ and CrO_4^{-}. An increase in the concentration of the chromate causes the hydrogel layer of the probe to shrink, and this results in an increase of its RI and a red shift of the resonance wavelength. The sensor covers a wide analytical range (from 10 pM to 1 μM) and has a 5 pM detection limit.

The anionic surfactant sodium dodecyl sulfate (SDS) can be sensed via fiber optics by using the cationic dye ethyl violet.[178] The cladding of a multimode fiber was removed, and ethyl violet was physically adsorbed on the core to form the sensing layer. The absorbance of the sensing layer decreases with an increase in the SDS concentration due to the formation of an ion pair. SDS can be quantified in the 4−15 mg/L concentration range with a moderate detection limit of 3.3 mg/L.

Salinity and Ionic Strength. Sensors for salinity and ionic strength are needed in marine sciences, during blood dialysis, in the chemical and nuclear industry in general, and in agriculture, in particular in arid areas. The salinity of water slightly affects its RI, and a refractometric FOCS was developed on the basis of this principle.[179] A mathematical model was developed to simulate the sensor response, and the concentration of NaCl in

DOI: 10.1021/acs.analchem.5b04298
Anal. Chem. 2016, 88, 203−227

water can be measured in the 0.02 to 0.5 M range. In a related sensing scheme, a whispering galley wave (WGW)-based sensor for salt concentration,[180] a WGW was induced in a macrobent optical fiber. The propagation of light changes as the RI in the replaced cladding area varies with salt concentration. On increasing the salt concentration from 1% to 25%, the WGW moves to longer wavelengths. By measuring the wavelength shift, the salt concentration can be determined in the range from 1% to 25%.

SENSORS FOR ORGANIC SPECIES

This chapter covers sensors (but not biosensors, which will be discussed in the next section) for organic species such as explosives, pollutants, agrochemicals, nerve agents, drugs, pharmaceuticals, gasoline, and oil. FOCS have wide potential applications in these fields because of their compact size. In fact, several portable devices have been developed for quick, quantitative, and partially real-time analysis. A portable UV (190−400 nm) spectrophotometric-based reflected FOCS was developed for on-site detection and identification of explosives (Figure 6) including the seven most common explosives, viz.,

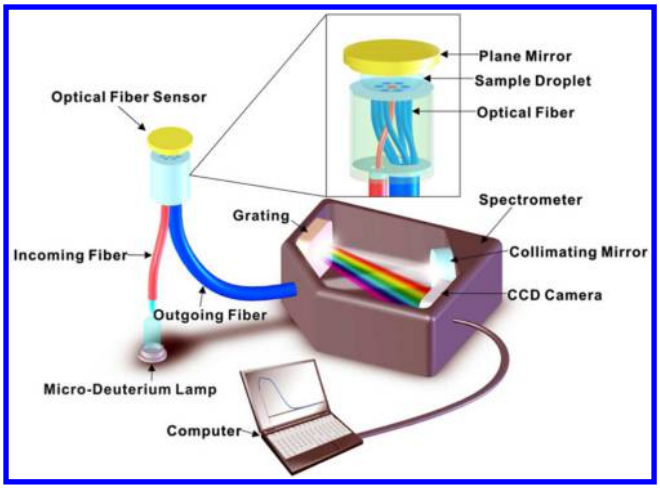

Figure 6. Schematic diagram of a portable UV spectrophotometric system for sensing explosives. (Reprinted from *Anal. Chim. Acta*, Vol. *751*, Li, X.; Li, Q.; Zhou, H.; Hao, H.; Wang, T.; Zhao, S.; Lu, Y.; Huang, G. Rapid, on-site identification of explosives in nanoliter droplets using a UV reflected fiber optic sensor, pp. 112−118 (ref 181). Copyright 2012, with permission from Elsevier).

pentaerythritol tetranitrate (PETN), trinitrophenylmethylnitramine (CE), trinitrotoluene (TNT), dinitrotoluene (DNT), picric acid (PA), cyclotetramethylenetetranitramine (HMX), and cyclotrimethylenetrinitramine (RDX), and a PETN−RDX mixture.[181] The device can quantitatively analyze and identify these explosives in less than 3 s with limits of detection of 0.3 mg/L. A feature-matching algorithm was used for the identification of the explosives to prevent chemical interferences in the UV range.

Many explosives have relatively high vapor pressure and can be smelled, especially by dogs. Various methods have been developed to detect vapor phase explosives such as TNT or RDX, for example, by placing gold nanoparticles on a U-shaped fiber-optic waveguide with a core diameter of 200 μm and bend diameter of 1.5 mm.[182] The gold nanoparticles were then functionalized with thiols such as 4-mercaptobenzoic acid, L-cysteine, or cysteamine to provide binding sites for the explosives. On binding to the nanoparticles, RI of the fiber coating is changed and this causes the SPR peak wavelength to be shifted. The evanescent field technique was applied to excite the localized SPR. This sensor is said to be highly selective for gaseous TNT, and the detection limit is in the ppb levels without preconcentration. Cennamo et al.[183] described an SPR-based optical sensor for TNT. It also uses a plastic optical fiber and can detect TNT in aqueous solution. The cladding of a plastic optical fiber was removed along half the circumference; the exposed core was spin coated with a photoresist, and a thin gold film was sputtering onto it. A TNT-imprinted polymer film was then deposited on the gold film. The results show that the upper polymer layer enables highly selective determination of TN, with a 50 μM detection limit (i.e., ∼11 μg per mL).

A U-shaped poly(methyl methacrylate) optical fiber was coated with a fluorescent porous thin film and used for sensing vapor phase explosives.[184] Porphyrin, which acts as the molecular reporter, was covalently immobilized on a polyhedral oligomeric silsesquioxane (POSS-V8) via click chemistry. Vapor phase explosives exert a strong quenching effect on the fluorescence of the porphyrin. Even trace quantities of TNT (10 ppb), DNT (180 ppb), and nitrobenzene (315 ppb) can be detected in <30 s. An ultrasensitive optical sensor for explosives relies on a chemomechanically prepared polymer-incorporated fiber interferometer.[185] A fiber Fabry-Pérot interferometer was coated with poly(4-vinylpyridine), which induces cavity expansion upon adsorption of vapors of nitrobenzene and other nitroaromatics, and this shifts the phase matching condition of the resonating modes. The detection limit is as low as 5 ppb (v/v). However, it takes 18−20 min to analyze a sample which is not fast enough for real-time monitoring or screening of explosives. Standard techniques such as those based on ion mobility spectrometry still appear to perform much better.

Glucose Sensing. This section covers sensors not based on the use of enzymes (which are treated in the "Enzymatic Biosensors" section). As reported several times in the past, glucose concentrations can be directly quantified with fiber-optic systems by using attenuated total reflection (ATR).[186,187] Such sensors are exploiting the typical absorption of glucose in the infrared. Previous sensors lacked selectivity because numerous other species also absorb at certain wavelength, and water can also interfere. By working at five laser wavelengths in the range from 1081 to 1037 cm^{-1}, glucose determination becomes more specific. The absorbance at the five wavelengths correlates well with glucose concentration in the range from 500 mg/L to 5 g/L, and the limit of detection is 38 mg/L. Sensitivity can be enhanced by using a U-shaped fiber-optic ATR sensor coated with silver nanoparticles.[188]

Boronic acid-based sensors are attractive due to their high affinity for saccharides. The current challenge is to make such sensors highly specific over fructose because fructose often is taken by diabetics as a replacement for glucose. Hence, the selectivity coefficients of sensors for clinical uses have to be higher than 50 (i.e., the signal for glucose has to be at least 50 times stronger than the signal for fructose present in the same concentration). An affinity-based glucose sensor was developed by replacing the cladding of the optic fiber with a layer of gold nanoparticle and an overcoating of a borate-functionalized polyacrylamide.[189] The binding of glucose to the borate polymer changes the surface RI of the sensor, and signal was readout by measuring the SPR absorbance. Glucose concentration in the range of 1−300 mg/dL can be accurately

DOI: 10.1021/acs.analchem.5b04298
Anal. Chem. 2016, 88, 203−227

determined, and the sensor shows high sensitivity at low concentration of glucose. Another boronic acid monolayer coating formed by 2-[(6-aminohexyl)−(benzyl)aminomethyl] phenylboronic acid (ABA-PBA) was found to result in a poor response to glucose and mannose, but to be well suited for sensing fructose in the 10−50 mM range.[190] A monolayer ABA-PBA was placed on the gold layer on the fiber core to form a fiber-optic SPR sensor. The interaction between the ABA-PBA monolayer and fructose induced the shift of resonance wavelength, which was used as analytical signal.

Sucrose. Sucrose in fruit juices can be determined[191] with an FOCS that was fabricated by coating a U-shaped optical fiber with a layer of gold nanoparticles and an overlayer of silicon nitride. Exposure of the sensor probe to sucrose affects its RI, and this causes a change in the transmittance of the fiber. The size of gold nanoparticles and the thickness of the silicon nitride layer determine sensitivity. Best performance sensing was found when using a coating composed of 39 nm diameter gold nanoparticles and a 20 nm silicon nitride film coating. Graphene oxide decorated with gold nanoparticles was coated onto the core of an optical fiber to produce a localized SPR sensor for sucrose.[192] Unfortunately, the sensor was not characterized in terms of analytical ranges and detection limit. A dendrimer was shown to be a viable "nano-glue" in an SPR-based sucrose sensor.[193] The unclad fiber core was first coated with a layer of dendrimer and then with a layer of gold nanoparticles. Coupling SPR and waveguide technologies results in excellent sensor tunability and self-referencing capability. The presence of a dielectric waveguide sandwiched between two metal layers allows for precise tuning of the resonance wavelength over a wide range (from visible to the near-infrared) and to generate multiple modes which may be selectively used for other applications. A waveguide coupled SPR sensor for sucrose was developed[194] on the basis of this principle. It exhibits enhanced performance and the detection is self-referenced which increases accuracy.

Oils. An SPR sensor was designed that can detect and quantify various kinds of oil in waste waters.[195] The sensor was constructed by coating the unclad core of a fiber waveguide with a layer of silver or gold. The sensor head was coated with a layer of silver that acts as a mirror. Depending on its content of oil, the RI of wastewater varies, and this induces a resonance wavelength shift if the sensing area is placed in the test solution. An increase in the concentration of oil in wastewater causes a longwave shift of the SPR wavelength. Another fiber-optic SPR sensor was described that can detect 3-pyridinecarboxamide (a.k.a. vitamin B3) by using a molecularly imprinted hydrogel.[196] The sensor relies on a spectral interrogation technique. SPR spectra were recorded for solutions of VitB3 in varying concentrations. They undergo a red shift on increasing the concentration of VitB3, which is due to binding of VitB3 to the specific receptor sites of the molecular imprint. The sensitivity (spectral shift per concentration change) is 1.483 nm per mg/mL. A fiber-optic long-period grating (LPG) can directly detect the adulteration of virgin olive oil[197] because both the RI and the resonance peak of the LPG change when the cladding surface of the fiber is exposed to adulterated oil. The sensor was repeatedly used to detect oil adulteration, with a detection limit of 4% of a common adulterating additive.

Other Organics. An unclad core on an optical fiber was used as the sensing region for direct evanescent wave-based sensing of the yellow-colored and clinically relevant metabolite bilirubin.[198] By choosing a wavelength corresponding to the bilirubin absorption peak (460 nm), the attenuation of the evanescent wave is related to the concentration of bilirubin. Preliminary results show that the sensor is capable of measuring the concentration of bilirubin, but sensitivity is rather low which was attributed to an incomplete removal of the fiber cladding.

A photonic crystal fiber (PCF) sensor based on modal interferometry was used for determining the concentration of glycerol in water.[199] Numerical analysis was employed for data analysis, and the resonant wavelength shift is related to the RI of the glycerol solution. The sensor has a linear response in the the 0.0−50% concentration range. The resonant wavelength shifts toward shorter wavelength with the increasing concentration of glycerol. Such sensors are, of course, not selective in that any compounds also changing the RI will interfere. Similarly, a tapered plastic optical fiber sensor for the Remazol black B dye in the textile manufacturing effluent[200] will be interfered by any other species also absorbing at around 600 nm. When immersed into a solution of Remazol black B dye solution, the evanescent wave absorbance can be used for quantifying dye concentration. The sensor has a linear response to dye concentration in the range from 0 to 70 ppm.

A very different sensing scheme was applied to determine melamine, an illegal additive formerly added to milk to increase its content of nitrogen.[201] The surface of the unclad core of an optical fiber was decorated with a layer of silver nanoclusters, and the adsorption of melamine on the silver layer causes a decrease of the evanescent wave absorbance. Melamine in the concentration range from 0 to 10 mg/mL can be measured with this arrangement, and the limit of detection is 1.0 μg/mL. Improved selectivity for melamine was achieved by applying the molecular imprinting (MIP) technique.[202] A layer of a melamine-MIP was deposited on a thin film of silver on the unclad core of an optical fiber representing an SPR sensor that works over the rather wide 10 μM to 0.1 M range.

A catalytic FOCS was developed that can detect the pollutant 2,4-dichlorophenol (DCP).[203] Iron(III) complex of tetrasulfophthalocyanine displays catalytic activity in accelerating the oxidation of DCP by oxygen. The quantity of oxygen consumed is proportional to the concentration of DCP and can be measured with a known oxygen optode based on the oxygen sensitive fluorescence lifetime probe $Ru(bipy)_3$. The sensor can quantify DCP in the concentration range from 1.0 to 9.0 μM, and the typical response time is 250 s. The sensor is fairly stable over time, and this allows it to be employed to the analysis of environmental samples. The same sensing system was later employed to measure the concentration of 2-chlorophenol.[204] Obviously, it is not highly selective.

Absorbance-based methods of analysis are often adversely affected by the turbidity of media. Scattering particles suspended in a sample therefore cause large errors. Evanescent wave-based sensing is much less interfered by turbidity than conventional absorptiometry (in cuvettes or microtiter plates) because the penetration depth of the evanescent wave typically is in the order of the wavelength of the interrogating light and does not "reach" the particles. Llorente et al.[205] demonstrated a U-shaped optical fiber arrangement for determination of the dye Toluidine Blue in highly turbid media. The cladding of the curved area of the fiber was removed to expose the fiber core and to enable the internally reflected light to evanesce. Monitored at the maximum absorption wavelength, the sensor can measure the dye in the concentration range of 0.5−5 μM with a detection limit of 0.5 μM.

DOI: 10.1021/acs.analchem.5b04298
Anal. Chem. 2016, 88, 203−227

The cancerogenic reagent *o*-phenylenediamine (OPD) can be fairly selectively determined by SERS using silver nanoparticles decorated with α-cyclodextrin.[206] The method is based on the chemical cyclization reaction of OPD with nitrite. Benzotriazole, one of the products of the reaction, can be determined by SERS with high sensitivity when using silver nanoparticles decorated with α-cyclodextrin (α-CD-AgNPs) as a substrate. The enhancement factors of the SERS substrates range from 2.17×10^6 to 2.52×10^6 when utilizing the SERS peak at 1602 cm^{-1}. Other figures of merit include a linear analytical range from 0.10 to 1.0 μmol L^{-1} OPD and a 30 nM detection limit.

BIOSENSORS

This section covers biosensors based on the use of antibodies, nucleic acids, aptamers, enzymes, and even whole cells. A large increase in the number of biosensors based on the use of aptamers (now readily available via the SELEX technique) is noted. Biosensors make use of biological components in order to sense a species of interest (which by itself need not be a "biospecies"). On the other side, chemical sensors not using a biological component but placed in a biological matrix (such as a pH electrode in blood) *are not biosensors* by definition. It should be noted that some of the biosensors can be found in other chapters if this was deemed to be more appropriate.

Nucleic Acid-Based Biosensors (DNA- and Aptamer-Based). Such bio"sensors" can be highly selective and have low limits of detection, but all respond irreversibly and therefore do not match the definition of sensors given at the beginning of this Review. It is, however, quite common to refer to devices containing immobilized biomolecules as "biosensors". An SPR-based FOCS was designed for the detection of single-nucleotide polymorphism (SNP), the smallest possible type of genetic variability.[207] A short chain of single-strand DNA (ssDNA) was immobilized on the surface of a fiber, and another short chain of ssDNA was immobilized on gold nanoparticles (AuNPs). Once the target (analyte) long-chain ssDNA is present in solution, it will hybridize with the short chain ssDNA, and a monolayer of AuNPs will assemble on the fiber surface. In the case of a mismatch, binding of analyte DNA to the AuNPs and, hence, on the SPR fiber will be affected, and this results in altered hybridization kinetics. By slowly heating the sample, the surface-bound DNA will melt and the AuNPs will detach from the sensor surface, causing an SPR wavelength shift. In addition, the melting temperatures of the duplexes formed with analyte ssDNA and with mismatched interference ssDNA are different.

Aptamers can be readily immobilized on fiber surfaces in order to construct aptasensors for targeting biomolecules.[208] An SPR-based sensor for thrombin protein was fabricated by coating the cladding of a tilted FBG with a 30−50 nm thick AuNP coating. The surface of the AuNPs was self-assembled with a monolayer of thrombin-binding aptamers via the established thiol−gold interaction. Binding of thrombin to the aptamer shifts the resonance wavelength to around 1550 nm, and this effect can be used to detect the protein. The sensor has an excellent selectivity for thrombin, while other proteins such as BSA do not interfere. Another aptasensor was designed[209] in order to detect the outer membrane proteins of *Escherichia coli* (EcOMPs). It uses a similar setup (i.e., long period gratings integrated into a single mode fiber) and covalently immobilized aptamers against EcOMPs. The recognition and binding of the EcOMPs by the aptamers alters the RI of the coating and causes a resonance wavelength shift of the evanescent wave. The EcOMPs can be detected in the concentration range between 0.1 and 10 nM, and the sensor can be regenerated by treatment with acid.

Immunosensors. These form a large class of biosensor, all responding practically irreversibly. A highly sensitive and selective optofluidics-based fluorescent immunosensor for measuring bisphenol A (BPA) was fabricated.[210] The capture molecular BPA−bovine serum albumin was covalently immobilized on the surface of the optical fiber. The working principle of the sensor is based on the competitive binding. A mixture of different concentrations of BPA and a certain concentration of fluorescently labeled anti-BPA monoclonal antibodies after prereaction was introduced to the optofluidic cell. A higher concentration of BPA reduced the fluorescently labeled antibodies bound to the fiber surface, and the fluorescence signal will be reduced. The sensor exhibits high sensitivity and selectivity, which can measure BPA in the range of 0.5−100 μg/L with a detection limit of 0.06 μg/L.

A highly sensitive label-free immunosensor was described[211] for detection of *Escherichia coli* B (*E. coli* B). Again, a long-period grating (LPG) was used that was coated with T4 bacteriophage adhesin protein (gp37). The adhesive phage protein was bound on the nickel ions immobilized on the LPG surface, and the protein could irriversibly bind to the *E. coli* B by recognizing its bacterial lipopolysaccharide. The binding event changes the RI of the fiber and induces the resonance wavelength shift, which can be used to measure the bacteria in real time and with high accuracy. An immunosensor based on localized SPR for detecting Dengue fever, in turn, uses a standard multimode fiber[212] whose distal end was coated with a layer of AuNPs onto which an antibody against the Dengue NS1 antigen was physically immobilized. The binding between antigen and antibody changes the extent of specular reflection and was used to determine the NS1 antigen. The sensor can detect NS1 antigen in the range of 0−1 μg/mL with a detection limit of 74 ng/mL and may be used for Dengue fever diagnosis in the acute phase of the infection. Localized SPR immunosensing was applied in a biosensor for γ-interferon, and the tumor marker prostate-specific antigen (PSA).[213] The antibody against γ-interferon was physically adsorbed on the AuNPs, which then were placed at the distal end of the optical fiber. The analytical range is from 2 to 500 pg/mL of PSA, and the limit of detection is 1 pg/mL. The results were compared to data obtained by localized SPR using dark-field spectroscopy. SPR-based immunosensing of human epidermoid carcinoma A431 (HECA431) cells and OCM1 cells was developed.[214] The unclad core of a tilted FBG was first coated with a layer of gold nanoparticles, followed by physically adsorbing monoclonal antibodies against the extracellular domain of epidermal growth factor receptors. The sensor works in the near-infrared wavelength (~1550 nm) which is favorable for detection of micrometer-size HECA431 and OCM1 cells. The fabricated sensor is highly sensitive and can detect a single intact HECA431 and OCM1 cell even in the presence of other cells at a concentration of 3×10^6 cells/mL.

The use of gold nanorods (AuNRs) rather than gold nanospheres strongly improves the performance of SPR-based immunosensors because AuNRs offer operation in the near-infrared window so that less interferences are observed in the case of colored samples. A respective sensor was designed[215] for label-free detection of orchid viruses. The AuNRs were immobilized on the surface of an unclad fiber core and then

DOI: 10.1021/acs.analchem.5b04298
Anal. Chem. 2016, 88, 203−227

functionalized with antibodies against *Cymbidium mosaic virus* or *Odontoglossum ringspot virus*. The detection limits for these two viruses in leaf saps were 48 and 42 pg/mL, respectively, which is much better than the limit of detection obtained by the ELISA approach (1200 pg/mL). Improved sensitivity also was achieved by replacing the gold nanospheres by hollow gold nanostructures (HAuNS).[216] A localized SPR-based immunosensor was developed using the HAuNS labeled with human immunoglobulin-G (HIgG) and coated on the unclad fiber core on the surface. The binding between the targeting molecules goat-anti-HIgG and the HIgG protein changes the RI, and this causes the absorbance at 640 nm to change. Goat-anti-HIgG protein can be detected in the 1 ng/mL to 10 μg/mL concentration range, which is around 1.5 times better than in the case of a sensor using gold nanospheres.

Optic fiber sensors are highly attractive in terms of point-of-care diagnostics. Sensors for glucose are highly attractive but are treated in other sections. Other parameters include blood lipids and uric acid. An SPR-based fiber-optic biosensor for low-density lipoprotein (LDL) was constructed by coating an unclad fiber core with a gold film, modifiying the gold film with a layer of 4-aminothiophenol, and finally depositing an overlayer of anti-apolipoprotein B.[217] The sensor shows high sensitivity and can quantify LDL in the range from 0 to 190 mg/dL within ~2 min.

A fiber-optic immunosensor for detection of Crimean-Congo hemorrhagic fever (CCHF) IgG antibodies[218] used the CCHF virus protein that was covalently immobilized on the unclad core of an optical fiber to form the sensor probe. By dipping the sensor probe into a patient's serum, the CCHF IgG antibody present in serum will bind to the sensor surface. Next, the sensor is immersed into a solution containing donkey antihuman IgG peroxidase-labeled antibodies. The peroxidase on the sensor surface can catalytically convert substrate and emit chemiluminescence (CL). The intensity of CL is related to the concentration of CCHF IgG antibody. Results showed that this CL immunosensor is 10 times more sensitive than the conventional colorimetric ELISA. Other bacterial pathogens can be detected in the same way. For example,[219] an optical waveguide carrying immobilized streptavidin was reacted with biotinylated polyclonal antibodies to immobilize the respective antibodies on the fiber surface. When the biofunctionalized FOCS was exposed to the food pathogens such as *Listeria monocytogenes*, *Escherichia coli O157:H7*, or *Salmonella enterica*, these bacteria were attached to the fiber surface and then could be detected after reaction with fluorescently labeled monoclonal secondary antibodies. These biosensors could detect each pathogen individually or in a mixture with very small cross-reactivity in meat samples. The detection limit was as low as ~10^3 cfu/mL for all three pathogens.

The clinically significant α-fetoprotein (AFP) was determined with an optical microfiber sandwich immunosensor.[220] The first antibody was immobilized on the unclad core of the optical fiber (as shown in Figure 7). On exposure to a sample containing AFP, it will bind to the surface. Next, the sensor is treated with secondary antibody labeled with AuNPs to form a sandwich. As a result, AuNPs will be present on the fiber's surface. The evanescent wave absorption of the AuNPs at 535 nm can be used to quantify AFP. Because the amplification effects the use of AuNPs, the detection limit of AFP is as low as 0.2 ng/mL in phosphate buffered saline and 2 ng/mL in the presence of bovine serum.

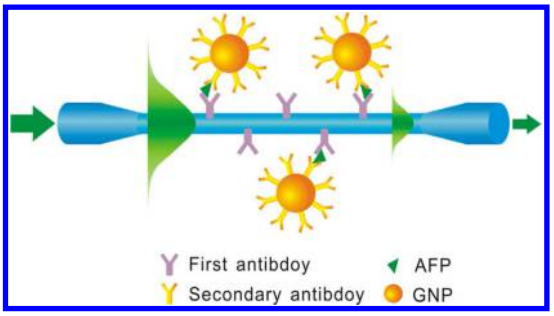

Figure 7. Schematic diagram of the immunoassay for α-fetoprotein (AFP) using gold nanoparticles as signal amplifying labels on the secondary antibody. (Reprinted from *Talanta*, Vol. *120*, Li, K.; Zhou, W.; Liu, G.; Hao, P.; Wu, Y.; Zhang, Z. Gold nanoparticle amplified optical microfiber evanescent wave absorption biosensor for cancer biomarker detection in serum, pp. 419–424 (ref 220). Copyright 2014, with permission from Elsevier).

Enzymatic Biosensors. Enzymatic reactions proceed with high efficiency and specificity and usually at temperatures below 50 °C. Glucose remains to be the main target in sensor development. It is interesting to note that, despite major efforts to develop nonenzymatic sensors for glucose, not a single one is on the market after almost 20 years of substantial research. Rather, practically all clinical sensors for glucose still are enzyme based. Most enzymatic sensors work at near-neutral pH values. An SPR-based fiber-optic enzymatic biosensor for glucose was fabricated by coating a fiber core with a sensing film composed of a silver layer, a silicon layer, and a gel layer containing immobilized glucose oxidase.[221] The SPR spectra undergo a blue shift in resonance wavelength with increasing concentration of glucose in samples. The sensor operates in the 0–2.6 g/L concentration range and also works in whole blood. Glucose oxidase (GOx) was covalently immobilized on a polyaniline (PAni) film using glutaraldehyde as the cross-linking reagent.[222] The PAni film was deposit on the unclad fiber core and used for glucose sensing. The refractive index (RI) of the modified cladding changes due to the oxidation of glucose by GOx, and this variation in RI changes the number of leaky modes coupled back to the core. The intensity modulation is inherently related to the glucose concentration. The sensing film is quite stable and highly reproducible, and this allowed for continuous sensing of glucose over a period of 36 days. The analytical range is up to 2 mM (which is below the glucose level in blood), and the detection limit is 10 nM.

An enzymatic SPR-based FOCS was developed for urea in liquid solution.[223] Again, an unclad fiber was properly modified, this time by coating it with layers of silver, silicon and, finally, a gel layer incorporating urease. Urease catalyzes the hydrolysis of urea to form ammonium ion and hydrogen carbonate. Wavelength interrogation was applied to characterize the sensor, and its resonance wavelength was found to decrease on increasing the concentration of urea. The sensor works in the 0–160 mM urea concentration range. An improved biosensor for ethanol was described that uses immobilized alcohol dehydrogenase and NAD^+ placed at the head of an optical fiber head in a sol–gel matrix.[224] Enzymatic dehydrogenation of ethanol produces NADH which causes the absorbance at around 350 nm to increase. The sensor can detect ethanol in the 2–18% (v/v) range with good sensitivity. It was applied to real-time monitoring of ethanol during wine production. The main advantage of this biosensor is its high selectivity. However, enzymatic ethanol sensors are more

DOI: 10.1021/acs.analchem.5b04298
Anal. Chem. 2016, 88, 203–227

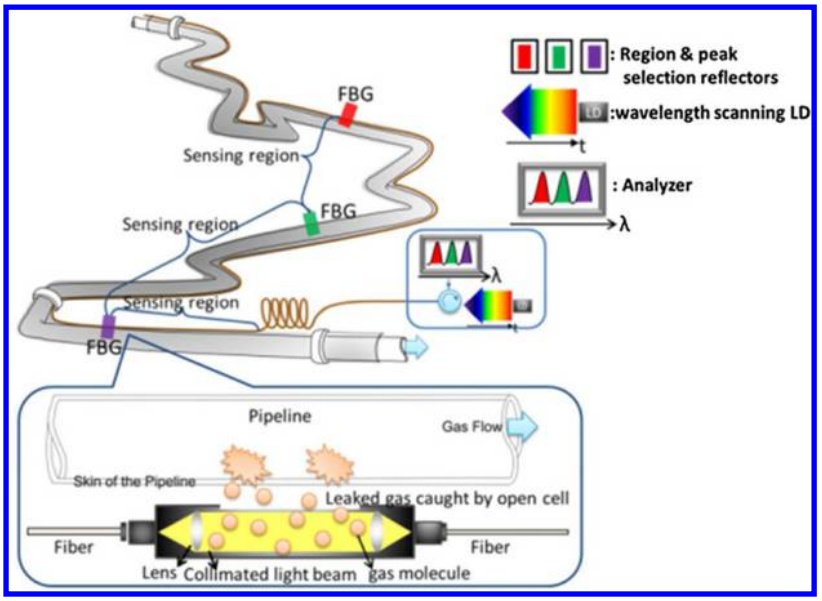

Figure 8. Conceptual schematic of fiber Bragg grating-based detection of gas leaks along a pipeline. (Reproduced with permission from Lu, M.; Nonaka, K.; Kobayashi, H.; Yang, J.; Yuan, L. *Meas. Sci. Technol.* **2013**, *24*, 095104 (ref 234). Copyright 2013, IOP Publishing Ltd.).

expensive than conventional refractometric sensors, and they sometimes suffer from long-term stability and high temperature dependence.

An SPR-based FOCS for the clinically significant triacylglycerides was described.[225] The enzyme lipase hydrolyzes triacylglycerides to form glycerol and fatty acids. It was immobilized on a silver-coated unclad portion of an optical fiber in a gel matrix. The sensor works based on the wavelength interrogation technique, and the shift in resonance wavelength of the transmission spectra is directly proportional to the concentration of triacylglycerides. Response is linear in the concentration range of 0.5−7.0 mM. Mitsubayashi and coworkers[226] developed a fluorescence-based enzymatic fiber-optic biosensor for measuring acetone concentration in exhaled breath. Sample breath gas was passed through a flow cell containing a sensor membrane incorporating NADH and alcohol dehydrogenase (which also metabolizes acetone). NADH is consumed in this reaction, and its consumption is proportional to the concentration of acetone vapor. As a result, the fluorescence of NADH increases, and this was used to determine acetone in the 20−5300 ppb (v/v) concentration range. Not unexpectedly, ethanol interferes. The same group[227] was making use of this principle in a fiber-optic biosensor for formaldehyde (FA) in indoor air. The sensor measures the fluorescence of reduced NADH produced during enzymatic oxidation of FA as catalyzed by FA dehydrogenase (FA-DH). In order to prevent the loss of enzyme activities in the gas phase, a microflow-cell with FA-DH-immobilized in a membrane was constructed. Under optimized conditions, the sensor is capable of measuring FA vapor at subppb levels, and the detection limit is as low as 750 ppt. The authors also demonstrated the use of the sensor to monitor the photocatalytic degradation of FA using TiO_2 particles. Verma and Gupta[228] recently described a fiber-optic SPR biosensor for ethanol. The unclad core of a multimode fiber was first coated with a 40 nm thin film of silver, and then, alcohol dehydrogenase and nicotinic acid were immobilized on the silver coating by a gel entrapment method. The biosensor can measure ethanol in the 0−10 mM concentration range in buffered pH 7 solutions.

Other Biosensors. A RI-based sensor for gelatin uses a single mode tapered fiber and is operated at 1550 nm.[229] When light in the fiber proceeds from the untapered regions into the tapered regions, the core modes and the fiber cladding modes are coupled, and the peak wavelength of the transmission spectrum can be related to the gelatin concentration in the range from 0 to 5% (w/v). An evanescent wave-based fiber-optic sensor was created[230] to monitor the growth and hydrogen production capability of biofilms. The sensor consists of two probes, one acting as a sensing probe, the other as a reference. The sensing probe consists of an etched fiber with rough surface. It can detect the formation of the biofilm by measuring changes in the evanescent wave absorbance of (photosynthetic) bacteria. The reference probe is coated with a Teflon membrane to separate the liquids from bacteria and to measure the RI of the liquid only (whose changes also may affect absorbance). Biofilms in thicknesses between 0 and 120 μm are detectable. The same sensing system was also used[231] for monitoring biomass growth in a photobioreactor.

■ NEW SCHEMES AND MATERIALS

This section covers both new spectroscopic sensing schemes and new materials because they often come together.

New Sensing Schemes. A highly interesting new gas sensing scheme was introduced by the group of Braud.[232] It is based on wavelength conversion in chalcogenide fibers doped with Er(III) ions. Incoherent IR light (wavelength 4.4 μm) is converted to NIR light (wavelength 810 nm) in erbium-doped GaGeSbS fibers and in bulk glass samples. This energy conversion is achieved by pumping the doped chalcogenide fibers at 982 nm and simultaneously exciting them with a 4.4 μm IR signal. This approach paved the way for the development of an "all-optical" absorptiometric gas sensor capable of detecting traces of gases using commercial silica fibers. A thermally stable mesoporous silica−titania (SiO_2−TiO_2) nanocomposite containing a pH indicator was shown[233] to represent an attractive alternative to sol-gel-based sensor

DOI: 10.1021/acs.analchem.5b04298
Anal. Chem. 2016, 88, 203−227

materials. It can be obtained by the sol–gel method. The indicator is homogeneously distributed in the pores of the network. Nitrogen adsorption isotherms demonstrated the mesoporous nature of the nanocomposite by showing a surface area of 401 m^2/g, a pore size of 3.3 nm, and a pore volume of 0.33 cm^3/g. Absorption spectroscopy revealed sensitivity to pH in the range from 3 to 5 with a response time of 6.9 s and to pH values around 12 within 1 s.

A new concept for sensing gases was introduced by Lu et al.[234] It is supposed to detect the types and locations of gas leakages at multiple regions over long distances. This distributed sensing technique measures the distinct absorption lines of each gas. The multiregion remote monitoring system contains an FBG monitor as the spectroscopy unit, long propagation fibers, gas cells at various sites in the sensing region, and FBGs as region selectors. This is schematically shown in Figure 8. By measuring both the wavelength and travel time, the location and type of leaking gas can be identified, for example, in long-distance pipelines.

The coupling of fiber-optic sensing technology to electrochemical detection represents another promising sensing scheme that can result in enhanced selectivity.[235] A sensor was fabricated by coating an unclad fiber core with a gold mesh, and attenuated total reflection was used as the optical detection mode. The electrochemical oxidation–reduction of an analyte at the electrode induces changes in the attenuation of light passing the fiber core (Figure 9). Methylene blue and

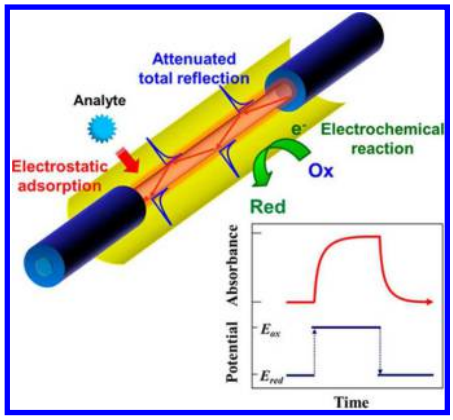

Figure 9. Sensing based on fiber-optic technology coupled to electrochemical detection is based on the measurement of the attenuation of light traveling along the fiber core as a result of electrochemical oxidation or reduction of an analyte. (Reproduced from Imai, K.; Okazaki, T.; Hata, N.; Taguchi, S.; Sugawara, K.; Kuramitz, H. *Anal. Chem.* **2015**, *87*, 2375 (ref 235). Copyright 2015, American Chemical Society).

ferrocyanide were used as model analytes to evaluate the performance of the sensor. The changes in optical transmission generated by redox reactions are linearly related to the concentrations of methylene blue and ferrocyanide, respectively, with 0.2 μM and 1.6 mM limits of detection. Proper selection of the working voltage improves selectivity, and ferrocyanide ions in simulated nuclear waste were determined by this method.

The group of Gangopadhyay[236] has modeled an optical fiber loop resonator and an evanescent field absorption sensor for use in chemical detection. The fiber loop cavity resonator is shown to undergo a shift of cavity resonance due to change of the RI of the external medium (water–isopropanol mixtures). Part 2 of the study describes the optimization of the parameters of the evanescent wave absorption with respect to sensor length (1–1.5 mm) and diameter (<20 μm) of an etched optical fiber. Experimental studies were performed with a 419 ppm solution of cobalt nitrate.

In designing the nanoparticle-based SPR sensors, AuNPs are commonly used, but the use of silver nanoparticles results in better sensitivity.[237] The chemical instability of metallic silver is a potential problem, but the deposition of an Ag_2O overlayer on the silver layer can solve the problem. The overlayer also increases sensitivity and causes a red shift of the resonance wavelength. On the other hand, the overlayer also broadens the SPR spectrum. Besides Ag_2O, zinc oxide was also used as the protecting layer for preventing the metallic layer from oxidation, and the resulting SPR sensor is more sensitive.[238] The sensitivity of an SPR-based fiber-optic sensor for RI was improved by placing an additional layer of oxides (of metals and nonmetals) on the gold film.[239] A typical configuration contains copper as the SPR-active layer and cover layers consisting of TiO_2, SiO_2, or SnO_2. Maximum sensitivity is found for the TiO_2 film. An increase in the thickness of the TiO_2 layer also increases sensitivity. The oxide layers also offer the additional advantages of (a) protecting the metal layer from oxidation, (b) tunability of the resonance wavelength, and (c) capability of gas sensing. The use of various gold–silver alloys in the SPR sensor was shown to enable fine-tuning of sensitivity.[240] In essence, an increase of the fraction of gold in the alloyed nanoparticles enhances sensitivity.

The unique electromagnetic and mechanical properties of graphene result in a continued interest in the use of this nanomaterial. Graphene layers can be used, for example, as a replacement for gold and silvers in SPR sensors.[241,242] The graphene film was synthesized by thermal chemical vapor deposition. The SPR signal changes according to the RI of the interface which, in turn, is governed by the analytes. Exemplarily, biotinylated DNA lattice and the protein streptavidin were used for evaluation. The same SPR phenomena as in case of using gold films were observed. Upconversion nanoparticles represent another class of highly attractive materials for use in optical (fiber) sensing. Spectrally matched upconverting luminescent nanoparticles were presented that enable monitoring of biochemical reactions involving the coenzyme FAD or the cosubstrate NADH because the emission of the nanoparticles matches the absorptions of these biomolecules.[243] Fluorescent nanoparticles also were found to allow for sensing and imaging of cellular oxygen via two-photon photoexcitation at 980 nm.[244]

A Fabry-Pérot optical fiber tip was coated with a thin film of polyelectrolyte multilayers via a layer-by-layer approach and used for measurements of RI.[245] Poly(diallyldimethylammonium chloride) and poly(sodium styrenesulfonate) were used as the polyelectrolytes. After being coating with this composite, the inflection point of the Fabry-Pérot tip sensor shifts from 1.457 to 1.4623, with a fringe contrast that is independent of temperature. This sensor design allows sensing of chemical and biological species via the RI change and can be used even at different (room) temperatures.

Molecularly Imprinted Polymer (MIP)-Based Sensors. Such sensors rely on the use of a polymer that has cavities of the size and shape of the analyte that may fit the cavity. MIPs sometimes were referred to as plastic immunoreceptors. The use of such materials can strongly improve selectivity and allows for working at fairly high temperatures. For example, a

DOI: 10.1021/acs.analchem.5b04298
Anal. Chem. 2016, 88, 203–227

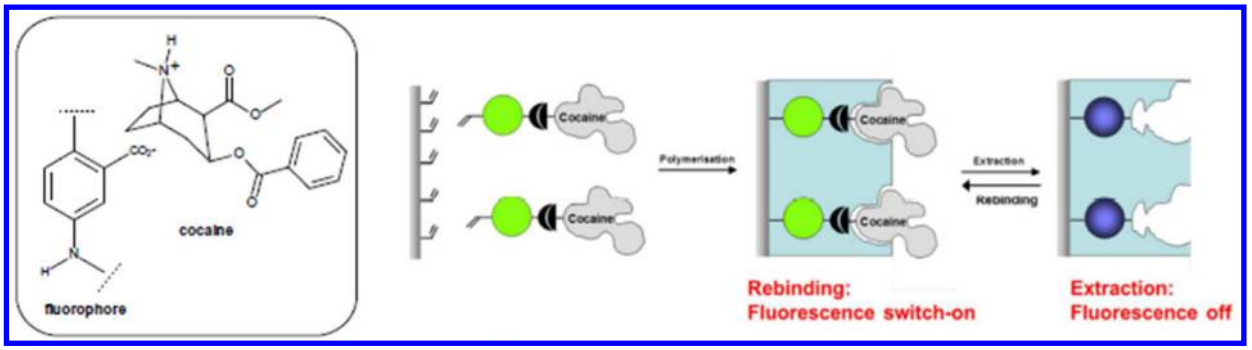

Figure 10. Scheme of the MIP sensor for cocaine detection. (Reprinted from Wren, S. P.; Nguyen, T. H.; Gascoine, P.; Lacey, D.; Sun, T.; Grattan, K. T. V. Preparation of a novel drug sensor using a molecular imprinted polymer approach, *Proc. SPIE* **2013**, *8794*, 879417 (ref 252) with the permission. Copyright 2013, Society of Photo-Optical Instrumentation Engineers).

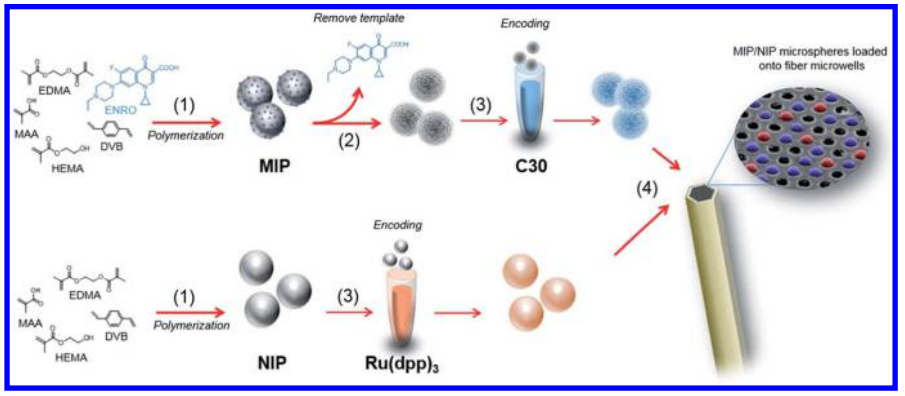

Figure 11. Workflow of microarray fabrication. (1) MIP microspheres selective to ENRO and nonimprinted polymer (NIP) microspheres were prepared via a precipitation−polymerization approach. The NIPs are used as a control. (2) MIP microspheres are extensively washed until no template is washed out any longer. (3) MIP and NIP microspheres were then encoded with C30 and $[Ru(dpp)_3]Cl_2$. (4) A suspension of 0.25 mg mL^{-1} NIP and MIP microspheres was prepared in acetonitrile, and a drop of 1 mL of the suspension is deposited onto the etched distal end of the fiber. (Reprinted from Carrasco, S.; Benito-Pena, E.; Walt, D. R.; Moreno-Bondi, M. C. *Chem. Sci.* **2015**, *6*, 3139 (ref 254), with permission of The Royal Society of Chemistry).

MIP matrix was used in combination with an SPR sensor to fabricate an FOCS for tetracycline in food.[246,247] A thin film of silver metal was placed on the unclad region of an optical fiber core, and a layer of MIP was deposited over the metal coating. The interaction of tetracycline with the binding site in the MIP results in the changes in the dielectric properties (i.e., the RI) of the sensing surface, which induces the shift in the SPR spectrum toward the red region. The sensor can measure tetracycline in the 0−0.96 μM concentration range and possesses high selectivity for tetracyclines. This technique also was used in an SPR sensor to detect 3-pyridinecarboxamide (vitamin B_3) in the 1−10 mg/L concentration range. Korposh et al.[248] have deposited MIP nanoparticles on an optical fiber long-period grating (LPG) and demonstrated the ability to use such a sensor for detection of the antibiotic vancomycin which was selected as the molecular target. The sensor is based on the measurement of changes in RI as induced by the binding of vancomycin by the nano-MIPs deposited on the cladding of the LPG. Concentration as low as 10 nM can be precisely quantified, and high selectivity over other antibiotics such as amoxicillin, bleomycin, and gentamicin was observed.

MIP technology also was combined with Bragg grating-based fiber sensing of small molecules.[249] The sensor uses an imprint for maltol and has a surprisingly low detection limit of 1 ng/mL only. In related work, a microvolume MIP-based FOCS was reported for the food pollutant bisphenol A (BPA) by evanescent wave fluorometry.[250] The MIP layer was placed on the fiber core and further inserted into a transparent capillary to form a microvolume sensor. BPA is selectively adsorbed on the MIP film and thereby preconcentrated on the fiber surface. UV light is used to evanescently excite the purple fluorescence of BPA whose intensity is related to the concentration of BPA in the range from 3 to 5000 ng/mL. In closely related work, an evanescent-wave-based MIP-based fiber-optic sensor for the textile dye Basic Red 9 (that occur in textile effluents) was reported.[251] A layer of a MIP containing imprints for the dye was deposited on the optical waveguide. Basic red 9 binds readily to the MIP layer, and the intensity of color can be measured.

An interesting scheme was introduced where the MIP acts as both the molecular receptor and a fluorogenic reagent.[252] This was specifically demonstrated for the case of cocaine. A layer of a fluorescent MIP receptor was covalently bound to the distal end of an optical fiber (Figure 10). When cocaine enters the MIP receptor, a reaction occurs between the carboxy group of the fluorophore and the amino group of cocaine, and this turns on fluorescence. The concentration of cocaine is directly related to the enhancement of fluorescence. A strong increase in fluorescence is, however, observed at a rather high concentration (such as 1 mM) of cocaine only. This poor sensitivity presently limits its practicability. Another fluorescence enhancement (turn-on) assay was reported by the group of Haupt[253] who describe a disposable evanescent wave FOCS that uses a MIP containing signaling fluorophores. The MIP is composed

DOI: 10.1021/acs.analchem.5b04298
Anal. Chem. 2016, 88, 203−227

of a green emitting naphthalimide-based fluorophore that undergoes strong fluorescence enhancement on binding with molecules possessing carboxy groups, for example, the herbicide 2,4-dichlorophenoxyacetate and the mycotoxin citrinin. Both can be selectively and sensitively detected in the low nM concentration range. By manipulating the composition of the fluorescent monomers, a variety of carboxylated analytes can be sensed with good selectivity.

The Walt group had created a fiber-optic array using MIP microspheres for antibiotic analysis.[254] The sensor array was fabricated via chemically etching an optical fiber bundle containing approximately 50 000 individual fibers to create microwells, which was then filled with both red-fluorescently labeled MIP microspheres and blue-fluorescently encoded nonimprinted polymer (NIP) microspheres (Figure 11). The MIP microspheres had an imprint for the antibiotic enrofloxacin (ENRO). The methods works very much like a competitive immunoassay in that fluorescently labeled ENRO competes with unlabeled (analyte) ENRO for binding to the MIP. Strong fluorescence is observed if the concentration of the analyte (ENRO) is low. The limit of detection is 40 nM. The sensor array has excellent selectivity over similar fluoroquinolones which makes it an appropriate tool for the detection of ENRO in even complex samples.

Photonic Crystals. These are being increasingly used for purposes of chemical sensing and biosensing as demonstrated in a large review.[255] The use of photonic crystals, photonic crystal fibers, and hollow core Bragg fibers for gas sensing has been recently reviewed.[256] Such sensors respond to analytes by color changes that can be seen with bare eyes or read-out using mobile phone cameras based on RGB recording. The group of Russel[257] has reviewed the use of photonic crystal fibers (PhCFs) as optofluidic microdevices that can be employed as both a versatile chemical sensor and a highly efficient microreactor. PhCFs provide an excellent platform for quantitative spectroscopic analysis or photoactivation. PhCF-based sensing of gases and liquids is covered in some detail. These developments demonstrate that the tight light confinement, enhanced light−matter interaction, and reduced sample volume offered by PhCFs make it useful in a wide range of chemical applications. Examples include highly sensitive gas sensing by Raman spectroscopy in photonic crystal fibers[81] and photonic crystal fiber interferometry as a multifunctional sensor with a conceivably large potential in biosensing,[258] temperature-insensitive sensing of RI using a Fabry-Pérot cavity and a hollow-core photonic crystal fiber,[259] and an SPR sensor based on PhFs with metal nanolayers.[260] Many PhC fiber sensors for measurement of RI display a sensitivity that is comparable to that of conventional SPR. However, applications (such as for biosensing or high-throughput screening) are still in their infancy.

AUTHOR INFORMATION

Corresponding Authors

*E-mail: wangxudong@fudan.edu.cn. Tel: +86 21 6564 2790.
*E-mail: Otto.Wolfbeis@ur.de. Fax: +49 941 943 4064. Tel: +49 941 943 4065.

Notes

The authors declare no competing financial interest.

Biographies

Xu-dong Wang is a Full Professor in the department of chemistry at Fudan University (Shanghai, China). He received his PhD degree in Chemistry from Xiamen University (Xiamen, China) in 2011. He then worked as an Alexander von Humboldt fellow in the group of Prof. Wolfbeis at the University of Regensburg. After that, he joined Karlsruhe Institute of Technology in 2013 as a senior research scientist. In 2015, he was selected in the national "1000 Talents Program" in China and appointed as an "Eastern Scholar" distinguished Professor at Fudan University. His research interests are in the design of optical chemical and biosensors, in nanosensors and molecular probes, in developing novel (bio)sensing schemes, (nano)materials, and methods, and in their applications to biological and chemical analysis. He has authored or coauthored more than 30 articles in the past five years, and his current h-index is 16 (Oct. 2015).

Otto S. Wolfbeis was a Full Professor of Analytical and Interface Chemistry at the University of Regensburg, Germany, from 1995−2012. He has authored numerous papers and reviews on optical (fiber) chemical sensors, fluorescent probes, labels, and bioassays and on advanced (nano)materials for use in sensing schemes and in spectroscopic methods including fluorescence (lifetime) imaging. He has (co)edited several books and has acted as the (co)organizer of several conferences related to fluorescence spectroscopy (*MAF*) and to chemical sensors and biosensors (*Europtrode*). His h-index, according to Scholar Google, is 82 (Oct. 2015). He was one of the 10 editors of *Angewandte Chemie*, is the Editor-in-chief of *Microchimica Acta*, and one of the three editors of *Methods and Applications in Fluorescence*. Also see www.wolfbeis.de.

ACKNOWLEDGMENTS

This work was supported by the *Thousand Youth Talents Plan* of China and the *Program for Professor of Special Appointment* (Eastern Scholar) at Shanghai Institutions of Higher Learning (No. TP2014004). The TOC graphic was used with permission from Presens GmbH, Regensburg.

REFERENCES

(1) Wang, X.-D.; Wolfbeis, O. S. *Anal. Chem.* **2013**, *85*, 487 and earlier reviews cited therein..
(2) Wolfbeis, O. S. *Angew. Chem., Int. Ed.* **2013**, *52*, 9864.
(3) Klein, L. C. *Sol-gel optics: processing and applications*; Springer Science & Business Media: Berlin, 2013; Vol. *259*.
(4) Wang, X.-d.; Wolfbeis, O. S. *Chem. Soc. Rev.* **2014**, *43*, 3666.
(5) Zawawi, M. A.; O'Keffe, S.; Lewis, E. *Sens. Rev.* **2013**, *33*, 57.
(6) Caucheteur, C.; Guo, T.; Albert, J. *Anal. Bioanal. Chem.* **2015**, *407*, 3883.
(7) Wang, X.-d.; Wolfbeis, O. S.; Meier, R. J. *Chem. Soc. Rev.* **2013**, *42*, 7834.
(8) Edmonds, T. E. *Chemical sensors*; Springer Science & Business Media: Berlin, 2013.
(9) Wolfbeis, O. S. In *Optical Fiber Sensors*; Dakin, J., Culshaw, B., Eds.; Artech House: Boston-London, 1997; Vol. *IV*, p 53.
(10) Poole, Z. L.; Ohodnicki, P.; Chen, R.; Lin, Y.; Chen, K. P. *Opt. Express* **2014**, *22*, 2665.
(11) Alwis, L.; Sun, T.; Grattan, K. T. V. *Measurement* **2013**, *46*, 4052.
(12) Wang, X.-d.; Meier, R. J.; Schmittlein, C.; Schreml, S.; Schäferling, M.; Wolfbeis, O. S. *Sens. Actuators, B* **2015**, *221*, 37.
(13) Bhatia, P.; Gupta, B. D. *Proc. SPIE* **2012**, *8351*, 83511V.
(14) Javahiraly, N.; Perrotton, C.; Meyrueis, P.; Dam, B. *Proc. SPIE* **2013**, *8720*, 872004.
(15) Javahiraly, N.; Perrotton, C.; Slaman, M.; Dam, B.; Meyrueis, P. *Proc. SPIE* **2012**, *8368*, 836804.
(16) Perrotton, C.; Westerwaal, R. J.; Javahiraly, N.; Slaman, M.; Schreuders, H.; Dam, B.; Meyrueis, P. *Opt. Express* **2013**, *21*, 382.
(17) Hosoki, A.; Nishiyama, M.; Igawa, H.; Seki, A.; Choi, Y.; Watanabe, K. *Sens. Actuators, B* **2013**, *185*, 53.
(18) Gu, F.; Wu, G.; Zeng, H. *Nanoscale* **2015**, *7*, 924.

DOI: 10.1021/acs.analchem.5b04298
Anal. Chem. 2016, 88, 203−227

(19) Westerwaal, R. J.; Rooijmans, J. S. A.; Leclercq, L.; Gheorghe, D. G.; Radeva, T.; Mooij, L.; Mak, T.; Polak, L.; Slaman, M.; Dam, B.; Rasing, T. *Int. J. Hydrogen Energy* **2013**, *38*, 4201.
(20) Westerwaal, R. J.; Gersen, S.; Ngene, P.; Darmeveil, H.; Schreuders, H.; Middelkoop, J.; Dam, B. *Sens. Actuators, B* **2014**, *199*, 127.
(21) Mak, T.; Westerwaal, R. J.; Slaman, M.; Schreuders, H.; van Vugt, A. W.; Victoria, M.; Boelsma, C.; Dam, B. *Sens. Actuators, B* **2014**, *190*, 982.
(22) Ma, G. M.; Jiang, J.; Li, C. R.; Song, H. T.; Luo, Y. T.; Wang, H. B. *Rev. Sci. Instrum.* **2015**, *86*, 045003.
(23) Masuzawa, S.; Okazaki, S.; Maru, Y.; Mizutani, T. *Sens. Actuators, B* **2015**, *217*, 151.
(24) Ohodnicki, P. R.; Baltrus, J. P.; Brown, T. D. *Sens. Actuators, B* **2015**, *214*, 159.
(25) Dai, J.; Yang, M.; Yu, X.; Lu, H. *Opt. Fiber Technol.* **2013**, *19*, 26.
(26) Wang, M.; Yang, M.; Cheng, J.; Zhang, G.; Liao, C. R.; Wang, D. N. *IEEE Photonics Technol. Lett.* **2013**, *25*, 713.
(27) Chowdhury, S. A.; Correia, R.; Francis, D.; Brooks, S. J.; Jones, B. J. S.; Thompson, A. W. J.; Hodgkinson, J.; Tatam, R. P. *J. Lightwave Technol.* **2015**, *33*, 2535.
(28) Yu, C.; Liu, L.; Chen, X.; Liu, Q.; Gong, Y. *Photonic Sens.* **2015**, *5*, 142.
(29) Song, H.; Chen, Y.; Zhang, G.; Liu, Y.; Huang, P.; Zhao, H.; Yang, M.; Dai, J.; Li, Z. *Sens. Actuators, B* **2015**, *216*, 11.
(30) Liu, Y.; Chen, Y.-P.; Song, H.; Zhang, G. *IEEE Sens. J.* **2013**, *13*, 2699.
(31) Tabassum, R.; Gupta, B. D. *Appl. Opt.* **2015**, *54*, 1032.
(32) Szilágyi, P. A.; Westerwaal, R. J.; van de Krol, R.; Geerlings, H.; Dam, B. *J. Mater. Chem. C* **2013**, *1*, 8146.
(33) Li, Z.; Yang, M.; Dai, J.; Wang, G.; Huang, C.; Tang, J.; Hu, W.; Song, H.; Huang, P. *Sens. Actuators, B* **2015**, *206*, 564.
(34) Li, Z.; Zhou, C.; Deng, X.; Tang, Y. *Asian J. Chem.* **2014**, *26*, 5717.
(35) Kalanur, S. S.; Lee, Y.-A.; Seo, H. *RSC Adv.* **2015**, *5*, 9028.
(36) Yang, M.; Li, Z.; Dai, J.; Yang, Z.; Zhang, Y.; Zhuang, Z. *Meas. Sci. Technol.* **2013**, *24*, 094009.
(37) Yang, M.; Dai, J. *Photonic Sens.* **2014**, *4*, 300.
(38) Wang, Y.; Yang, M.; Zhang, G.; Dai, J.; Zhang, Y.; Zhuang, Z.; Hu, W. *J. Lightwave Technol.* **2015**, *33*, 2530.
(39) Dai, J.; Yang, M.; Yang, Z.; Li, Z.; Wang, Y.; Wang, G.; Zhang, Y.; Zhuang, Z. *Sens. Actuators, B* **2014**, *190*, 657.
(40) Jiang, H.; Yang, R.; Tang, X.; Burnett, A.; Lan, X.; Xiao, H.; Dong, J. *Sens. Actuators, B* **2013**, *177*, 205.
(41) Wang, S.-T.; Zhang, P.-W.; Zhu, Q.-M. *Key Eng. Mater.* **2013**, *562*−*565*, 1008.
(42) Shemshad, J. *Sens. Actuators, B* **2013**, *186*, 466.
(43) Schoonbaert, S. B.; Tyner, D. R.; Johnson, M. R. *Appl. Phys. B: Lasers Opt.* **2015**, *119*, 133.
(44) Shemshad, J. *Sens. Actuators, A* **2015**, *222*, 96.
(45) Mishra, S. K.; Tripathi, S. N.; Choudhary, V.; Gupta, B. D. *Plasmonics* **2015**, *10*, 1147.
(46) Martan, T.; Aubrecht, J.; Podrazky, O.; Matejec, V.; Kasik, I. *Sens. Actuators, B* **2014**, *202*, 123.
(47) Quaranta, M.; Borisov, S. M.; Klimant, I. *Bioanal Rev.* **2012**, *4*, 115.
(48) Xiong, Y.; Ye, Z.; Xu, J.; Zhu, Y.; Chen, C.; Guan, Y. *Analyst* **2013**, *138*, 1819.
(49) Chen, R.; Formenti, F.; McPeak, H.; Obeid, A. N.; Hahn, C. E. W.; Farmery, A. D. *IEEE Sens. J.* **2014**, *14*, 3358.
(50) Ongun, M. Z.; Oter, O.; Sabanci, G.; Ertekin, K.; Celik, E. *Sens. Actuators, B* **2013**, *183*, 11.
(51) Pulido, C.; Esteban, O. *Sens. Actuators, B* **2013**, *184*, 64.
(52) Yang, X.; Zheng, Y.; Luo, S.; Liu, Y.; Yuan, L. *Sens. Actuators, B* **2013**, *182*, 571.
(53) Kazemi, A. A.; Mendoza, E.; Goswami, K.; Kempen, L. *Proc. SPIE* **2013**, *8720*, 872002.
(54) Eich, S.; Schmaelzlin, E.; Loehmannsroeben, H.-G. *Sensors* **2013**, *13*, 7170.
(55) Chu, C.-S.; Lin, C.-A. *Sens. Actuators, B* **2014**, *195*, 259.
(56) Chu, C.-S.; Chuang, C.-Y. *Sens. Actuators, B* **2015**, *209*, 94.
(57) Lehner, P.; Staudinger, C.; Borisov, S. M.; Regensburger, J.; Klimant, I. *Chem. - Eur. J.* **2015**, *21*, 3978.
(58) Larndorfer, C.; Borisov, S. M.; Lehner, P.; Klimant, I. *Analyst* **2014**, *139*, 6569.
(59) Zhao, H.; Zang, L.; Wang, L.; Qin, F.; Zhang, Z.; Cao, W. *Sens. Actuators, B* **2015**, *215*, 405.
(60) Chaturvedi, P.; Hauser, B. A.; Foster, J. S.; Karplus, E.; Levine, L. H.; Coutts, J. L.; Richards, J. T.; Vanegas, D. C.; McLamore, E. S. *Sens. Actuators, B* **2014**, *196*, 71.
(61) Medina-Rodriguez, S.; de la Torre-Vega, A.; Fernandez-Sanchez, J. F.; Fernandez-Gutierrez, A. *Sens. Actuators, B* **2013**, *176*, 1110.
(62) Lehner, P.; Staudinger, C.; Borisov, S. M.; Klimant, I. *Nat. Commun.* **2014**, *5*, 4460.
(63) Kochmann, S.; Baleizão, C.; Berberan-Santos, M. N.; Wolfbeis, O. S. *Anal. Chem.* **2013**, *85*, 1300.
(64) Zhang, T.; Wang, X.; Wei, Y.; Wang, C.; Liu, T. *Appl. Mech. Mater.* **2013**, *278*−*280*, 983.
(65) Jozdani, M. M.; Khorsandi, A.; Sabouri, S. G. *Appl. Phys. B: Lasers Opt.* **2015**, *118*, 219.
(66) Kim, G.-j.; Choi, B.; Choi, I. *Proc. SPIE* **2014**, *9044*, 90440C.
(67) Nwaboh, J. A.; Hald, J.; Lyngso, J. K.; Petersen, J. C.; Werhahn, O. *Appl. Phys. B: Lasers Opt.* **2013**, *110*, 187.
(68) Gouveia, C.; Balogh, K.; Baptista, J. M.; Kovacs, B.; Jorge, P. A. S. *Proc. SPIE* **2012**, *8421*, 84216L.
(69) Balogh, K.; Jesus, J. M.; Gouveia, C.; Domingues, J. O.; Markovics, A.; Baptista, J. M.; Kovacs, B.; Pereira, C. M.; Borges, M.-T.; Jorge, P. A. S. *Proc. SPIE* **2013**, *8785*, 8785FC.
(70) Wild, P. M.; Fyles, T. M.; Risk, D. A.; Sinton, D. A.; Bao, B.; Melo, L.; Jun, M. B. G.; Burton, G. European Patent WO2015061886A1, 2015; 26 pp.
(71) Dang, X.; Hu, H.; Wang, S.; Hu, S. *Microchim. Acta* **2015**, *182*, 455.
(72) Ding, L.; Fan, C.; Huang, J.; Liang, B.; Yuan, F.; Gong, D. *Proc. SPIE* **2012**, *8421*, 84218U.
(73) Ding, L.; Fan, C.; Zhong, Y.; Li, T.; Huang, J. *Sens. Actuators, B* **2013**, *185*, 70.
(74) Bueno, A.; Caucheteur, C.; Lahem, D.; Debliquy, M. *Sensors* **2015**, *15*, 9870.
(75) Cao, Y.; Jin, W.; Ho, H. L.; Ma, J. *Opt. Lett.* **2013**, *38*, 434.
(76) Usha, S. P.; Mishra, S. K.; Gupta, B. D. *Sens. Actuators, B* **2015**, *218*, 196.
(77) Mishra, S. K.; Rani, S.; Gupta, B. D. *Sens. Actuators, B* **2014**, *195*, 215.
(78) Tabassum, R.; Mishra, S. K.; Gupta, B. D. *Phys. Chem. Chem. Phys.* **2013**, *15*, 11868.
(79) Tabassum, R.; Mishra, S. K.; Gupta, B. D. *Proc. SPIE* **2013**, *8794*, 87941E.
(80) Zhou, H.; Wen, J.-Q.; Zhang, X.-Z.; Wang, W.; Feng, D.-Q.; Wang, Q.; Jia, F. *Phys. Procedia* **2014**, *56*, 1102.
(81) Yang, X.; Chang, A. S. P.; Chen, B.; Gu, C.; Bond, T. C. *Sens. Actuators, B* **2013**, *176*, 64.
(82) Renganathan, B.; Sastikumar, D.; Raj, S. G.; Ganesan, A. R. *Opt. Commun.* **2014**, *315*, 74.
(83) Renganathan, B.; Ganesan, A. R. *Opt. Fiber Technol.* **2014**, *20*, 48.
(84) Jarzebinska, R.; Korposh, S.; James, S.; Batty, W.; Tatam, R.; Lee, S.-W. *Anal. Lett.* **2012**, *45*, 1297.
(85) Manivannan, S.; Saranya, A. M.; Renganathan, B.; Sastikumar, D.; Gobi, G.; Park, K. C. *Sens. Actuators, B* **2012**, *171*−*172*, 634.
(86) Renganathan, B.; Sastikumar, D.; Srinivasan, R.; Bose, A. C.; Ganesan, A. R. *Asian J. Chem.* **2013**, *25*, S373.
(87) Renganathan, B.; Sastikumar, D.; Srinivasan, R.; Ganesan, A. R. *Mater. Sci. Eng., B* **2014**, *186*, 122.
(88) Mishra, S. K.; Tripathi, S. N.; Choudhary, V.; Gupta, B. D. *Sens. Actuators, B* **2014**, *199*, 190.

DOI: 10.1021/acs.analchem.5b04298
Anal. Chem. 2016, 88, 203−227

(89) Sansone, L.; Malachovska, V.; La Manna, P.; Musto, P.; Borriello, A.; De Luca, G.; Giordano, M. *Sens. Actuators, B* **2014**, *202*, 523.
(90) Kavinkumar, T.; Manivannan, S. *Ceram. Int.* **2015**, *42*, 1769.
(91) Huang, Y.; Wieck, L.; Tao, S. *Atmos. Environ.* **2013**, *66*, 1.
(92) Mishra, S. K.; Bhardwaj, S.; Gupta, B. D. *IEEE Sens. J.* **2015**, *15*, 1235.
(93) Bhatia, P.; Gupta, B. D. *Plasmonics* **2013**, *8*, 779.
(94) Rodríguez, A. J.; Zamarreno, C. R.; Matias, I. R.; Arregui, F. J.; Dominguez Cruz, R. F.; May-Arrioja, D. A. *Sensors* **2014**, *14*, 4060.
(95) Aubrecht, J.; Kalvoda, L. *Proc. SPIE* **2013**, *8774*, 877417.
(96) Ibrahim, S. A.; Rahman, N. A.; Abu Bakar, M. H.; Girei, S. H.; Yaacob, M. H.; Ahmad, H.; Mahdi, M. A. *Opt. Express* **2015**, *23*, 2837.
(97) Mariammal, R. N.; Ramachandran, K.; Renganathan, B.; Sastikumar, D. *Sens. Actuators, B* **2012**, *169*, 199.
(98) Sharifpour-Boushehri, S.; Hosseini-Golgoo, S. M.; Sheikhi, M.-H. *Opt. Fiber Technol.* **2015**, *24*, 93.
(99) Dhanuskodi, S.; Mohandoss, R.; Renganathan, B.; Sastikumar, D. *Opt. Laser Technol.* **2014**, *64*, 204.
(100) Noel, J. L.; Udayabhaskar, R.; Renganathan, B.; Muthu Mariappan, S.; Sastikumar, D.; Karthikeyan, B. *Spectrochim. Acta, Part A* **2014**, *132*, 634.
(101) Stella, C.; Soundararajan, N.; Ramachandran, K. *J. Mater. Sci.: Mater. Electron.* **2015**, *26*, 4178.
(102) Shabaneh, A. A.; Girei, S. H.; Arasu, P. T.; Rashid, S. A.; Yunusa, Z.; Mahdi, M. A.; Paiman, S.; Ahmad, M. Z.; Yaacob, M. H. *IEEE Photonics J.* **2014**, *6*, article no. 6802910.
(103) Shabaneh, A.; Girei, S.; Arasu, P.; Mahdi, M.; Rashid, S.; Paiman, S.; Yaacob, M. *Sensors* **2015**, *15*, 10452.
(104) Shobin, L. R.; Renganathan, B.; Sastikumar, D.; Park, K. C.; Manivannan, S. *IEEE Sens. J.* **2014**, *14*, 1238.
(105) Yang, H.-Z.; Qiao, X.-G.; Ali, M. M.; Islam, M. R.; Lim, K.-S. *J. Lightwave Technol.* **2014**, *32*, 1777.
(106) Aziz, A.; Lim, H. N.; Girei, S. H.; Yaacob, M.H.; Mahdi, M. A.; Pandikumar, A.; A, P. *Sens. Actuators, B* **2015**, *206*, 119.
(107) Karacali, T.; Hasar, U. C.; Ozbek, I. Y.; Oral, E. A.; Efeoglu, H. *J. Lightwave Technol.* **2013**, *31*, 295.
(108) Zhang, Z. H.; Lockwood, R.; Veinot, J. G. C.; Meldrum, A. *Sens. Actuators, B* **2013**, *181*, 523.
(109) Elosua, C.; Vidondo, I.; Arregui, F. J.; Bariain, C.; Luquin, A.; Laguna, M.; Matias, I. R. *Sens. Actuators, B* **2013**, *187*, 65.
(110) Some, S.; Xu, Y.; Kim, Y.; Yoon, Y.; Qin, H.; Kulkarni, A.; Kim, T.; Lee, H. *Sci. Rep.* **2013**, *3*, 1868.
(111) Niu, L.; Zhao, C.-L.; Kang, J.; Jin, S.; Guo, J.; Wei, H. *Opt. Commun.* **2014**, *313*, 243.
(112) Echeverria, J. C.; de Vicente, P.; Estella, J.; Garrido, J. J. *Talanta* **2012**, *99*, 433.
(113) Khan, M. R. R.; Kang, S.-W. *Sensors* **2014**, *14*, 23321.
(114) Lee, J.-S.; Yoon, N.-R.; Kang, B.-H.; Lee, S.-W.; Gopalan, S.-A.; Jeong, H.-M.; Lee, S.-H.; Kwon, D.-H.; Kang, S.-W. *Sensors* **2014**, *14*, 11659.
(115) Khan, M. R. R.; Kang, B.-H.; Yeom, S.-H.; Kwon, D.-H.; Kang, S.-W. *Sens. Actuators, B* **2013**, *188*, 689.
(116) Bahrampour, A.; Iadicicco, A.; De Luca, G.; Giordano, M.; Borriello, A.; Cutolo, A.; Cusano, A.; Scolaro, L. M. *Proc. SPIE* **2013**, *8794*, 87941N.
(117) Dong, L.; Deng, C.; He, C.; Shi, L.; Fu, Y.; Zhu, D.; Cao, H.; He, Q.; Cheng, J. *Sens. Actuators, B* **2013**, *180*, 28.
(118) Renganathan, B.; Ganesan, A. R. *Int. J. ChemTech Res.* **2015**, *7*, 878.
(119) Pan, Y.; Guo, X.; Zhu, J.; Wang, X.; Zhang, H.; Kang, Y.; Wu, T.; Du, Y. *Microchim. Acta* **2015**, *182*, 1775.
(120) Caponero, M. A.; Polimadei, A.; Benussi, L.; Bianco, S.; Colafranceschi, S.; Passamonti, L.; Piccolo, D.; Pierluigi, D.; Russo, A.; Felli, F.; Saviano, G.; Vendittozzi, C. *J. Instrum.* **2013**, *8*, T03003.
(121) Wang, H.; Guo, H.; Xiao, G.; Mrad, N.; Kazemi, A.; Ban, D. *Proc. SPIE* **2013**, *8720*, 872019.
(122) Lin, Y.; Gong, Y.; Wu, Y.; Wu, H. *Photonic Sens.* **2015**, *5*, 60.
(123) Zhang, Z. F.; Zhang, Y. *Opt. Laser Technol.* **2015**, *74*, 16.
(124) Churenkov, A. V. *Tech. Phys. Lett.* **2013**, *39*, 723.
(125) Egalon, C. O. *Proc. SPIE* **2013**, *8847*, 88471H.
(126) Mohd Noor, M. Y.; Khalili, N.; Peng, G. D. *Meas. Sci. Technol.* **2013**, *24*, 085203.
(127) Urrutia, A.; Goicoechea, J.; Rivero, P. J.; Matias, I. R.; Arregui, F. J. *Sens. Actuators, B* **2013**, *176*, 569.
(128) Batumalay, M.; Harun, S. W.; Irawati, N.; Ahmad, H.; Arof, H. *IEEE Sens. J.* **2015**, *15*, 1945.
(129) Harith, Z.; Irawati, N.; Rafaie, H. A.; Batumalay, M.; Harun, S. W.; Nor, R. M.; Ahmad, H. *IEEE Sens. J.* **2015**, *15*, 845.
(130) Wang, X.; Zhao, C.-L.; Li, J.; Jin, Y.; Jin, S. *Rev. Sci. Instrum.* **2013**, *84*, 043114.
(131) Zhang, S.; Dong, X.; Li, T.; Chan, C. C.; Shum, P. P. *Opt. Commun.* **2013**, *303*, 42.
(132) Yang, M.; Xie, W.; Dai, Y.; Lee, D.; Dai, J.; Zhang, Y.; Zhuang, Z. *Opt. Express* **2014**, *22*, 11892.
(133) Alwis, L.; Sun, T.; Grattan, K. T. V. *Sens. Actuators, B* **2013**, *178*, 694.
(134) Batumalay, M.; Harun, S. W.; Ahmad, F.; Nor, R. M.; Zulkepely, N. R.; Ahmad, H. *J. Mod. Opt.* **2014**, *61*, 244.
(135) Xiao, Y.; Zhang, J.; Cai, X.; Tan, S.; Yu, J.; Lu, H.; Luo, Y.; Liao, G.; Li, S.; Tang, J.; Chen, Z. *Opt. Express* **2014**, *22*, 31555.
(136) Ohira, S.-I.; Miki, Y.; Matsuzaki, T.; Nakamura, N.; Sato, Y.-k.; Hirose, Y.; Toda, K. *Anal. Chim. Acta* **2015**, *886*, 188.
(137) Løkken, T. V. *J. Nat. Gas Sci. Eng.* **2013**, *12*, 13.
(138) Løkken, T. V. *J. Nat. Gas Sci. Eng.* **2012**, *6*, 24.
(139) Løkken, T. V. *J. Nat. Gas Sci. Eng.* **2012**, *7*, 7.
(140) Cho, T.-S.; Choi, K.-S.; Seo, D.-C.; Kwon, I.-B.; Lee, J.-R. *Sensors* **2012**, *12*, 10906.
(141) Xiong, F.; Zhu, W.; Lin, H. *Appl. Mech. Mater.* **2013**, *303*−*306*, 59.
(142) Xiong, F. B.; Zhu, W. Z.; Meng, X. G.; Lin, H. F.; Huang, X. H.; Huang, Y. Q. *Optik* **2013**, *124*, 2008.
(143) Xiong, F. B.; Zhu, W. Z.; Lin, H. F.; Meng, X. G. *Appl. Phys. B: Lasers Opt.* **2014**, *115*, 129.
(144) Fenzl, C.; Hirsch, T.; Wolfbeis, O. S. *Sensors* **2012**, *12*, 16954.
(145) Huang, D.; Bing, Y.; Yi, H.; Hong, W.; Lai, C.; Guo, Q.; Niu, C. *Anal. Methods* **2015**, *7*, 4621.
(146) Bhatia, P.; Yadav, P.; Gupta, B. D. *Sens. Actuators, B* **2013**, *182*, 330.
(147) Tagad, C. K.; Dugasani, S. R.; Aiyer, R.; Park, S.; Kulkarni, A.; Sabharwal, S. *Sens. Actuators, B* **2013**, *183*, 144.
(148) Botero-Cadavid, J. F.; Wild, P.; Djilali, N. *Electrochim. Acta* **2014**, *129*, 416.
(149) Singh, S.; Gupta, B. D. *Sens. Actuators, B* **2012**, *173*, 268.
(150) Chiang, C.-C.; Hsu, C.-H.; Ou, C.-H. *Appl. Mech. Mater.* **2013**, *284*−*287*, 2157.
(151) Wong, W. C.; Chan, C. C.; Hu, P.; Chan, J. R.; Low, Y. T.; Dong, X.; Leong, K. C. *Sens. Actuators, B* **2014**, *191*, 579.
(152) Zhou, B.; Yang, S.; Nguyen, T. H.; Sun, T.; Grattan, K. T. V. *IEEE Sens. J.* **2014**, *14*, 1313.
(153) Schyrr, B.; Pasche, S.; Scolan, E.; Ischer, R.; Ferrario, D.; Porchet, J.-A.; Voirin, G. *Sens. Actuators, B* **2014**, *194*, 238.
(154) Islam, S.; Rahman, R. A.; Othaman, Z. B.; Riaz, S.; Naseem, S. *J. Ind. Eng. Chem.* **2015**, *23*, 140.
(155) Wang, C.; Ohodnicki, P. R.; Su, X.; Keller, M.; Brown, T. D.; Baltrus, J. P. *Nanoscale* **2015**, *7*, 2527.
(156) Zhao, Q.; Yin, M.; Zhang, A. P.; Prescher, S.; Antonietti, M.; Yuan, J. *J. Am. Chem. Soc.* **2013**, *135*, 5549.
(157) Henning, P. E.; Geissinger, P. *Meas. Sci. Technol.* **2012**, *23*, 045104.
(158) Henning, P. E.; Rigo, M. V.; Geissinger, P. *Sci. World J.* **2012**, *2012*, 876106.
(159) Yang, Q.; Wang, H.; Lan, X.; Cheng, B.; Chen, S.; Shi, H.; Xiao, H.; Ma, Y. *Sens. Actuators, B* **2015**, *207*, 571.
(160) Schwarze, T.; Mueller, H.; Ast, S.; Steinbrueck, D.; Eidner, S.; Geissler, F.; Kumke, M. U.; Holdt, H.-J. *Chem. Commun.* **2014**, *50*, 14167.

DOI: 10.1021/acs.analchem.5b04298
Anal. Chem. 2016, 88, 203−227

(161) Liu, Z.; Tonnele, C.; Battagliarin, G.; Li, C.; Gropeanu, R. A.; Weil, T.; Surin, M.; Beljonne, D.; Lazzaroni, R.; Debliquy, M.; Renoirt, J.-M.; Muellen, K. *J. Phys. Chem. B* **2014**, *118*, 309.
(162) Cheng, F.; Xu, H.; Wang, C.; Gong, Z.; Tang, C.; Fan, M. *RSC Adv.* **2014**, *4*, 64683.
(163) Kopitzke, S.; Geissinger, P. *Sensors* **2014**, *14*, 3077.
(164) Sung, T.-W.; Lo, Y.-L. *Sens. Actuators, B* **2012**, *165*, 119.
(165) Palai, G.; Mudului, N.; Sahoo, S. K.; Tripathy, S. K.; Patanaik, S. K. *Soft Nanosci. Lett.* **2013**, *3*, 16.
(166) Fenzl, C.; Kirchinger, M.; Hirsch, T.; Wolfbeis, O. S. *Chemosensors* **2014**, *2*, 207.
(167) Tabassum, R.; Gupta, B. D. *Sens. Actuators, B* **2015**, *220*, 903.
(168) Verma, R.; Gupta, B. D. *Food Chem.* **2015**, *166*, 568.
(169) Xing, X.; Yang, H.; Tao, M.; Zhang, W. *J. Hazard. Mater.* **2015**, *297*, 207.
(170) Bhavsar, K.; Prabhu, R.; Pollard, P. *J. Phys.: Conf. Ser.* **2013**, *450*, 012011.
(171) Liu, X.; Liu, X.; Tao, M.; Zhang, W. *J. Mater. Chem. A* **2015**, *3*, 13254.
(172) Crosby, J. S.; Lucas, D.; Koshland, C. P. *Sens. Actuators, B* **2013**, *181*, 938.
(173) Ma, J.; Chiniforooshan, Y.; Hao, W.; Bock, W. J.; Wang, Z. Y. *Proc. SPIE* **2013**, *8915*, 89151I.
(174) Yildirim, N.; Long, F.; He, M.; Gao, C.; Shi, H.-C.; Gu, A. Z. *Talanta* **2014**, *129*, 617.
(175) Venkataraj, R.; Nampoori, V. P. N.; Radhakrishnan, P.; Kailasnath, M. *IEEE Sens. J.* **2015**, *15*, 5584.
(176) Yahyavi, H.; Kaykhaii, M.; Mirmoghaddam, M. *Crit. Rev. Anal. Chem.* **2015**, 00.
(177) Mishra, S. K.; Gupta, B. D. *Anal. Methods* **2014**, *6*, 5191.
(178) Okazaki, T.; Imai, K.; Sultana, A.; Hata, N.; Taguchi, S.; Kuramitz, H. *Anal. Lett.* **2015**, *48*, 2217.
(179) Patil, S. S.; Shaligram, A. D. *J. Sens. Technol.* **2013**, *3*, 70.
(180) Chiang, C.-C.; Chao, J.-C. *J. Nanomater.* **2013**, *2013*, 372625.
(181) Li, X.; Li, Q.; Zhou, H.; Hao, H.; Wang, T.; Zhao, S.; Lu, Y.; Huang, G. *Anal. Chim. Acta* **2012**, *751*, 112.
(182) Bharadwaj, R.; Mukherji, S. *Sens. Actuators, B* **2014**, *192*, 804.
(183) Cennamo, N.; D'Agostino, G.; Galatus, R.; Bibbò, L.; Pesavento, M.; Zeni, L. *Sens. Actuators, B* **2013**, *188*, 221.
(184) Ma, J.; Lv, L.; Zou, G.; Zhang, Q. *ACS Appl. Mater. Interfaces* **2015**, *7*, 241.
(185) Bae, M.-K.; Lim, J. A.; Kim, S.; Song, Y.-W. *Opt. Express* **2013**, *21*, 2018.
(186) Yu, S.; Li, D.; Chong, H.; Sun, C.; Yu, H.; Xu, K. *Biomed. Opt. Express* **2014**, *5*, 275.
(187) Yu, S.; Li, D.; Chong, H.; Sun, C.; Xu, K. *Proc. SPIE* **2013**, *8591*, 85910K.
(188) Li, D.; Yu, S.; Sun, C.; Zou, C.; Yu, H.; Xu, K. *Biosens. Bioelectron.* **2015**, *72*, 370.
(189) Li, D.; Wu, J.; Wu, P.; Lin, Y.; Sun, Y.; Zhu, R.; Yang, J.; Xu, K. *Sens. Actuators, B* **2015**, *213*, 295.
(190) Qian, S.; Liang, Y.; Ma, J.; Zhang, Y.; Zhao, J.; Peng, W. *Sens. Actuators, B* **2015**, *220*, 1217.
(191) Chauhan, S. K.; Punjabi, N.; Sharma, D. K.; Mukherji, S. *Sens. Actuators, B* **2016**, *222*, 1240.
(192) Nayak, J. K.; Parhi, P.; Jha, R. *Sens. Actuators, B* **2015**, *221*, 835.
(193) Satija, J.; Mukherji, S. *Appl. Nanosci.* **2012**, *2*, 293.
(194) Ahn, J. H.; Seong, T. Y.; Kim, W. M.; Lee, T. S.; Kim, I.; Lee, K.-S. *Opt. Express* **2012**, *20*, 21729.
(195) Jiang, X.; Meng, Q. *Adv. Mater. Res.* **2013**, *850−851*, 1372.
(196) Verma, R.; Gupta, B. D. *Sens. Actuators, B* **2013**, *177*, 279.
(197) Libish, T. M.; Bobby, M. C.; Linesh, J.; Mathew, S.; Pradeep, C.; Nampoori, V. P. N.; Biswas, P.; Bandyopadhyay, S.; Dasgupta, K.; Radhakrishnan, P. *Laser Phys.* **2013**, *23*, 045112.
(198) Babin, S. M.; Sova, R. M. *Anal. Chem. Insights* **2014**, *9*, 59.
(199) Huang, J.; Li, X.; Yang, J. *Proc. SPIE* **2013**, *9044*, 90440S.
(200) Chong, S. S.; Abdul Aziz, A. R.; Harun, S. W.; Arof, H. *Sensors* **2014**, *14*, 15836.
(201) Luo, J.; Yao, J.; Wang, W.-m.; Zhuang, X.-y.; Ma, W.-y.; Lin, Q. *Proc. SPIE* **2013**, *8914*, 891412.
(202) Shrivastav, A. M.; Mishra, S. K.; Gupta, B. D. *Sens. Actuators, B* **2015**, *212*, 404.
(203) Tong, Y.; Li, D.; Huang, J.; Zhang, C.; Li, K.; Ding, L. *Bull. Korean Chem. Soc.* **2013**, *34*, 3307.
(204) Gong, J.; Huang, X.; Huang, J.; Ding, L.; Li, K.; Yuan, Y. *J. Wuhan Univ. Technol., Mater. Sci. Ed.* **2014**, *29*, 1178.
(205) Llorente, V. B.; Erro, E. M.; Baruzzi, A. M.; Iglesias, R. A. *Sens. Actuators, B* **2015**, *216*, 316.
(206) Ma, P.; Liang, F.; Wang, D.; Yang, Q.; Cao, B.; Song, D.; Gao, D.; Wang, X. *Microchim. Acta* **2015**, *182*, 167.
(207) Knez, K.; Janssen, K. P. F.; Pollet, J.; Spasic, D.; Lammertyn, J. *Small* **2012**, *8*, 868.
(208) Albert, J.; Lepinay, S.; Caucheteur, C.; Derosa, M. C. *Methods* **2013**, *63*, 239.
(209) Queiros, R. B.; Gouveia, C.; Fernandes, J. R. A.; Jorge, P. A. S. *Biosens. Bioelectron.* **2014**, *62*, 227.
(210) Long, F.; Zhu, A.; Zhou, X.; Wang, H.; Zhao, Z.; Liu, L.; Shi, H. *Biosens. Bioelectron.* **2014**, *55*, 19.
(211) Brzozowska, E.; Smietana, M.; Koba, M.; Gorska, S.; Pawlik, K.; Gamian, A.; Bock, W. J. *Biosens. Bioelectron.* **2015**, *67*, 93.
(212) Camara, A. R.; Gouvea, P. M. P.; Dias, A. C. M. S.; Braga, A. M. B.; Dutra, R. F.; de Araujo, R. E.; Carvalho, I. C. S. *Opt. Express* **2013**, *21*, 27023.
(213) Jeong, H.-H.; Erdene, N.; Park, J.-H.; Jeong, D.-H.; Lee, H.-Y.; Lee, S.-K. *Biosens. Bioelectron.* **2013**, *39*, 346.
(214) Malachovska, V.; Ribaut, C.; Voisin, V.; Surin, M.; Leclere, P.; Wattiez, R.; Caucheteur, C. *Anal. Chem.* **2015**, *87*, 5957.
(215) Lin, H.-Y.; Huang, C.-H.; Lu, S.-H.; Kuo, I. T.; Chau, L.-K. *Biosens. Bioelectron.* **2014**, *51*, 371.
(216) Satija, J.; Tharion, J.; Mukherji, S. *RSC Adv.* **2015**, *5*, 69970.
(217) Verma, R.; Srivastava, S. K.; Gupta, B. D. *IEEE Sens. J.* **2012**, *12*, 3460.
(218) Algaar, F.; Eltzov, E.; Vdovenko, M. M.; Sakharov, I. Y.; Fajs, L.; Weidmann, M.; Mirazimi, A.; Marks, R. S. *Anal. Chem.* **2015**, *87*, 8394.
(219) Ohk, S.-H.; Bhunia, A. K. *Food Microbiol.* **2013**, *33*, 166.
(220) Li, K.; Zhou, W.; Liu, G.; Hao, P.; Wu, Y.; Zhang, Z. *Talanta* **2014**, *120*, 419.
(221) Singh, S.; Gupta, B. D. *Sens. Actuators, B* **2013**, *177*, 589.
(222) Pahurkar, V. G.; Tamgadge, Y. S.; Gambhire, A. B.; Muley, G. G. *Sens. Actuators, B* **2015**, *210*, 362.
(223) Bhatia, P.; Gupta, B. D. *Sens. Actuators, B* **2012**, *161*, 434.
(224) Tarca, R. C.; Caraban, A. M.; Bota, S.; Tarca, I. C.; Dergez, A.; Cozma, A. C. *Rev. Chim.* **2014**, *65*, 1238.
(225) Baliyan, A.; Bhatia, P.; Gupta, B. D.; Sharma, E. K.; Kumari, A.; Gupta, R. *Sens. Actuators, B* **2013**, *188*, 917.
(226) Ye, M.; Chien, P.-J.; Toma, K.; Arakawa, T.; Mitsubayashi, K. *Biosens. Bioelectron.* **2015**, *73*, 208.
(227) Kudo, H.; Yamashita, T.; Miyajima, K.; Arakawa, T.; Mitsubayashi, K. *IEEE Sens. J.* **2013**, *13*, 2828.
(228) Verma, R.; Gupta, B. D. *Proc. SPIE* **2014**, *8992*, 89920A.
(229) Yadav, T. K.; Narayanaswamy, R.; Abu Bakar, M. H.; Kamil, Y. M.; Mahdi, M. A. *Opt. Express* **2014**, *22*, 22802.
(230) Zhong, N.; Liao, Q.; Zhu, X.; Chen, R. *Anal. Chem.* **2014**, *86*, 3994.
(231) Zhong, N.; Liao, Q.; Zhu, X.; Zhao, M. *Appl. Opt.* **2015**, *54*, 228.
(232) Pelé, A.; Braud, A.; Doualan, J.; Chahal, R.; Nazabal, V.; Boussard-Plédel, C.; Bureau, B.; Moncorgé, R.; Camy, P. *Opt. Express* **2015**, *23*, 4163.
(233) Islam, S.; Bidin, N.; Riaz, S.; Rahman, R. A.; Naseem, S.; Marsin, F. M. *Sens. Actuators, B* **2015**, *221*, 993.
(234) Lu, M.; Nonaka, K.; Kobayashi, H.; Yang, J.; Yuan, L. *Meas. Sci. Technol.* **2013**, *24*, 095104.
(235) Imai, K.; Okazaki, T.; Hata, N.; Taguchi, S.; Sugawara, K.; Kuramitz, H. *Anal. Chem.* **2015**, *87*, 2375.

DOI: 10.1021/acs.analchem.5b04298
Anal. Chem. 2016, 88, 203−227

(236) Linslal, C. L.; Syam Mohan, P. M.; Halder, A.; Gangopadhyay, T. K. *Sens. Actuators, A* **2013**, *194*, 160.
(237) Ciprian, D.; Hlubina, P. *Proc. SPIE* **2012**, *8697*, 86971N.
(238) Shukla, S.; Sharma, N. K.; Sajal, V. *Sens. Actuators, B* **2015**, *206*, 463.
(239) Singh, S.; Mishra, S. K.; Gupta, B. D. *Sens. Actuators, A* **2013**, *193*, 136.
(240) Tu, H.; Sun, T.; Grattan, K. T. *IEEE Sens. J.* **2013**, *13*, 2192.
(241) Kim, J. A.; Kulkarni, A.; Kang, J.; Amin, R.; Choi, J.-B.; Park, S. H.; Kim, T. *J. Nanosci. Nanotechnol.* **2012**, *12*, 5381.
(242) Kim, J. A.; Hwang, T.; Dugasani, S. R.; Amin, R.; Kulkarni, A.; Park, S. H.; Kim, T. *Sens. Actuators, B* **2013**, *187*, 426.
(243) Wilhelm, S.; del Barrio, M.; Heiland, J.; Himmelstoß, S. F.; Galbán, J.; Wolfbeis, O. S.; Hirsch, T. *ACS Appl. Mater. Interfaces* **2014**, *6*, 15427.
(244) Wang, X.-d.; Achatz, D. E.; Hupf, C.; Sperber, M.; Wegener, J.; Bange, S.; Lupton, J. M.; Wolfbeis, O. S. *Sens. Actuators, B* **2013**, *188*, 257.
(245) Jiang, M.; Li, Q.-S.; Wang, J.-N.; Yao, W.-G.; Jin, Z.; Sui, Q.; Shi, J.; Zhang, F.; Jia, L.; Dong, W.-F. *J. Lightwave Technol.* **2013**, *31*, 2321.
(246) Verma, R.; Gupta, B. D. *Analyst* **2013**, *138*, 7254.
(247) Shrivastav, A. M.; Mishra, S. K.; Gupta, B. D. *Mater. Res. Express* **2015**, *2*, 035007.
(248) Korposh, S.; Chianella, I.; Guerreiro, A.; Caygill, S.; Piletsky, S.; James, S. W.; Tatam, R. P. *Analyst* **2014**, *139*, 2229.
(249) Lepinay, S.; Ianoul, A.; Albert, J. *Talanta* **2014**, *128*, 401.
(250) Xiong, Y.; Ye, Z.; Xu, J.; Liu, Y.; Zhang, H. *Anal. Bioanal. Chem.* **2014**, *406*, 2411.
(251) Foguel, M. V.; Ton, X.-A.; Zanoni, M. V. B.; Sotomayor, M. D. P. T.; Haupt, K.; Tse Sum Bui, B. *Sens. Actuators, B* **2015**, *218*, 222.
(252) Wren, S. P.; Nguyen, T. H.; Gascoine, P.; Lacey, D.; Sun, T.; Grattan, K. T. V. *Proc. SPIE* **2013**, *8794*, 879417.
(253) Ton, X.-A.; Acha, V.; Bonomi, P.; Tse Sum Bui, B.; Haupt, K. *Biosens. Bioelectron.* **2015**, *64*, 359.
(254) Carrasco, S.; Benito-Pena, E.; Walt, D. R.; Moreno-Bondi, M. C. *Chem. Sci.* **2015**, *6*, 3139.
(255) Fenzl, C.; Hirsch, T.; Wolfbeis, O. S. *Angew. Chem., Int. Ed.* **2014**, *53*, 3318.
(256) Zhang, Y.-n.; Zhao, Y.; Bai, L.; Zhang, F. *Instrum. Sci. Technol.* **2013**, *41*, 187.
(257) Cubillas, A. M.; Unterkofler, S.; Euser, T. G.; Etzold, B. J. M.; Jones, A. C.; Sadler, P. J.; Wasserscheid, P.; Russell, P. S. J. *Chem. Soc. Rev.* **2013**, *42*, 8629.
(258) Cárdenas-Sevilla, G.; FáVero, F. C.; Villatoro, J. *Sensors* **2013**, *13*, 2349.
(259) Wang, Y.; Wang, D.; Liao, C.; Hu, T.; Guo, J.; Wei, H. *Opt. Lett.* **2013**, *38*, 269.
(260) Lu, Y.; Hao, C.-J.; Wu, B.-Q.; Musideke, M.; Duan, L.-C.; Wen, W.-Q.; Yao, J.-Q. *Sensors* **2013**, *13*, 956.

DOI: 10.1021/acs.analchem.5b04298
Anal. Chem. 2016, 88, 203−227